THE ROLE OF LIM HOMEODOMAIN TRANSCRIPTION FACTOR 1 IN SUPRACHIASMATIC NUCLEUS DEVELOPMENT AND CIRCADIAN FUNCTION

By Joseph L. Bedont

A dissertation submitted to Johns Hopkins University in conformity with the requirements for the degree of Doctor of Philosophy

Baltimore, Maryland

October, 2015

TITLE: **The Role of LIM Homeodomain Transcription Factor 1 in Suprachiasmatic Nucleus Development and Circadian Function**

Ph.D. Dissertator: Joseph L. Bedont

Ph.D. Advisor: Seth Blackshaw, Ph.D.

ABSTRACT

The suprachiasmatic nucleus (SCN) is the central light-entrained oscillator in mammals, transducing luminance input from the environment into holistic organism-wide coordination of cellular clocks on the solar time-scale. Yet despite this critical role, SCN development was poorly understood; at the beginning of my thesis, not a single transcription factor directly involved in its specification or differentiation was known. During my tenure, work from several labs has begun the long process of dissecting the transcriptional network controlling this process, including my thesis work on Lim homeodomain transcription factor 1 (Lhx1). Lhx1 is essential for terminal differentiation of several cell populations in the developing SCN, with an especially important role in promoting the expression of key SCN-enriched genes involved in signal transduction, including neuropeptide transmitters and their receptors and second messengers. Furthermore, through Vip signaling, Lhx1 indirectly controls the expression of numerous other SCN-enriched genes, including additional neuropeptides, among other actors. These transcriptional relationships give rise to a number of circadian phenotypes in *Six3-Cre;Lhx1*$^{lox/lox}$ mutants that lack Lhx1 in the developing SCN. Some phenotypes, like reduced synchronization of local cellular clocks in the SCN and wheel-running behavior, appear to be a result primarily of Lhx1's control of Vip expression. Others, such as the

near flattening of sleep rhythms and susceptibility to temperature entrainment by fever, appear to be critically reliant on Lhx1-controlled but Vip-independent gene expression lost in our mutants. In the process of investigating these questions, my collaborators and I have also gained novel and valuable insights into adult SCN physiology, which include the first *in vivo* cannulation data demonstrating previously unknown synergies among SCN neuropeptide signals, as well as the first direct *in vivo* evidence supporting a role for the SCN in the robustness of behavioral rhythms in the face of thermal insults. It is our hope that these findings, among others, clearly communicate the value of approaching adult circadian physiology from a developmental perspective.

Thesis Dissertation Committee

Seth Blackshaw, Ph.D.

Samer Hattar, Ph.D.

Jeremy Nathans, M.D., Ph.D.

Randall Reed, Ph.D.

ACKNOWLEDGEMENTS

"It takes a village to raise a child."

-African proverb

…And it takes a city to train a Ph.D. Coming into graduate school, I imagined that my thesis work would be more-or-less my and my mentor's task, perhaps with some help from within the lab. I could not have been more wrong. Among the many lessons learned and skills honed during my time at Johns Hopkins, the biggest imprint my graduate career has left me with is a marked penchant for diving into collaborative science, stretching my boundaries with friends inside the lab and out while helping them do the same, where I can.

First and foremost, I owe this and so much more to my incredible mentor, Dr. Seth Blackshaw. Seth takes the collaborativeness common at Hopkins and amplifies it to the nth degree, an approach I plan to shamelessly mimic as my own career develops in hopes of replicating some measure of his success. More generally, I cannot thank him enough for the ever-open door and mind he has given to my ever-cycling Crazy Ideas of the Week, nor for the judicious criticism he's used to help me refine my approach to problems and harness my scientific ADHD into more of an asset than a distraction. And most importantly, his endless enthusiasm for science and encouragement to keep fighting the good fight have been an inspiration for me, both in academia and in life.

Of course, just as critical to my growth in grad school were my supportive and occasionally wacky comrades-in-science on Team Blackshaw. Thank you all, but particularly Thuzar Thein, Liz Newman, Dan Lee, Sooyeon Yoo, Brian Clark, and Kai

Liu, not only for the collaborations and/or casual help we've pretty much all shared at one time or another, but more importantly for the good times that make it a pleasure to sit down at the bench every day. And I would like to especially thank our wonderful lab manager Hong Wang for her constant assistance with genotyping and other logistics for my thesis work, and for conducting the pilot studies that gave me a huge head start on my thesis project. Also, many thanks to my proximal rotation mentor Dan Lee and, conversely, my trainees Liz Newman, Travis Faust, and especially Abhi Bathini, for lessons learned on both ends of what it means to mentor someone in the lab.

I also want to extend my heartfelt thanks to my many (many, many…) collaborators, without whom my work would have been much diminished. Most importantly, I would like to thank my unofficial second mentor Dr. Samer Hattar and his team at Homewood as a whole for making their lab my scientific home-away-from-home throughout my tenure at Johns Hopkins, and especially Tara LeGates, Bill Keenan, Alan Rupp, and Diego Fernandez for collaborations and/or technical guidance for various experiments. I also want to heartily thank all the other collaborators who contributed to my thesis work: Dr. Mardi Byerly, Dr. Will Wong, Jon Ling, Dr. Phil Wong, Dr. Jianfei Hu, Dr. Jiang Qian, Dr. Dan Wu, and Dr. Jiangyang Zhang at Johns Hopkins; Emily Slat and Dr. Erik Herzog at Washington University in St. Louis; Dr. Ethan Buhr and Dr. Russ Van Gelder at the University of Washington; and Dr. Valerie Mongrain at the University of Montreal. Additionally, I would like to thank the collaborators who I have worked with on other projects, especially Ben Bell, Dr. Qili Liu, and Dr. Mark Wu at Johns Hopkins; Marlene Freyburger and Dr. Valerie Mongrain at the University of Montreal;

and Kwang Wook Min and Dr. Jin Woo Kim at the Korea Advance Institute of Science and Technology.

I would also like to thank the many faculty and staff in the Department of Neuroscience for their openness and generosity with their time. In particular, I would like to thank Drs. Samer Hattar, Jeremy Nathans, and Randall Reed for taking the time out of their busy schedules to serve on my thesis committee, and Drs. Nicholas Marsh-Armstrong, Michael Caterina, and Randall Reed for allowing me to rotate through their labs as a wee first-year. And I want to heartily thank Rita Ragan and Beth Woodroig, the fantastic administrative staff without whom the department would burn down inside a week, for acting as us grad students' "moms away from home" and making the Johns Hopkins bureaucracy infinitely easier to navigate.

I have also been enormously grateful for the teaching experiences I've had during my Ph.D. tenure, which have been an undeniably important supplement to my scientific education. I would like to thank Drs. Christine Hohmann and Michael Koban for the opportunity to design and teach my workshop at Morgan State, and Wendy Xin for keeping it going. I would also like to thank Drs. Erika Matunis, Douglas Robinson, and Miho Iijima for giving me the opportunity to work with the medical students in their Cell Physiology core course, and Drs. Seth Blackshaw and Samer Hattar for letting me co-teach with them at Homewood. Additionally, I would like to thank Daniel Pham, Delia Silva, Gabby Sell, and Chanel Matney for their help working together to re-vamp the neuroscience department's NSF GRFP fellowship workshop. Finally, I would like to thank Daniel Pham for giving me free rein to run the scientist training component of his outreach group Project Bridge, and Richard Sima for succeeding me in that post.

And of course, I would like to thank the many incredible friends I've made at Hopkins (apologies for not being able to list all of you; y'all are so awesome that my acknowledgements would never end). Without the game nights and weekend adventures, a cappella and science commiserating, and most important the banter, companionship, and support from all of you, my time in Baltimore would have been a truly sad and jading endeavor. Y'all shall be heartily missed, and I look forward to visiting often with my post-doc close by.

Finally, a tremendous thank you to my family, especially my parents Robert and Brenda Bedont. Without your unwavering support for my bookishness and weirdness, sensible laying down of boundaries, and instilling me with good old-fashioned blue-collar values growing up, I have no doubt that I would never have made it from the village to the city. All that I have and will become is very much a tribute to your love and support. So thank you, for everything.

Joseph L. Bedont

Johns Hopkins School of Medicine

October 2015

TABLE OF CONTENTS

List of Figures

List of Tables

1.1 Background and Significance

The central light-entrained circadian clock in mammals has been known to reside in the suprachiasmatic nucleus (SCN) of the hypothalamus since the 1970's, when daily rhythms in locomotor activity, drinking behavior, and hormone secretion were shown to be disrupted by SCN lesion (Moore and Eichler, 1972; Stephan and Zucker, 1972). In the 40-odd years since, our understanding of adult SCN function has moved beyond these purely phenotypic beginnings. Veritable mountains of papers have been published on the make-up of the molecular clockworks in the SCN and elsewhere in the body, the importance of SCN neurotransmitters for synchronizing these internal clocks with the solar day, and the retinal and other inputs to the SCN that impinge upon this internal signal transduction (reviewed in Buhr and Takahashi, 2013; Slat et al, 2013). However, the field's understanding of how this elegant system develops has badly lagged understanding of the adult network. Until the last few years, mostly descriptive studies of developmental phenomenology such as neurogenesis dates of SCN neurons and the timing of neuropeptide induction had been published; the transcriptional mechanisms choreographing this process were virtually unknown (reviewed in Bedont and Blackshaw, 2015).

This dissertation focuses on the elucidation of one such factor's role in this developmental process and (consequently) adult SCN function: Lim homeomain transcription factor 1 (Lhx1). Chapter 1 will summarize modern understanding of adult SCN physiology, the older phenomenological literature on SCN development, and the handful of studies on other transcription factors published before my work, setting the stage for the rest of my thesis. Chapter 2 will focus on my investigation of

developmental defects in the *Lhx1*-deficient SCN, while Chapter 3 will describe our efforts to characterize circadian defects in *Six3-Cre;Lhx1*$^{lox/lox}$ mutants. Chapter 4 will then synthesize these findings and discuss their import for the broader developmental and circadian fields, as well as discuss future directions.

1.2 Literature Review

Large parts of this chapter are direct excerpts and/or paraphrased passages from Bedont and Blackshaw, 2015 and Blackshaw et al, 2015.

1.2.1 Adult SCN Function

Since the initial identification of the SCN as the seat of the master circadian clock, our understanding of its function has grown dramatically. Perhaps most importantly, the molecular clock that drives time-keeping on a cellular level has to a large extent been worked out. At its core, a Bmal1/Clock heterodimer drives expression of Per and Cry genes, which feed back to inhibit their own transcription and whose expression levels thus communicate solar time to the cell (reviewed in Buhr and Takahashi, 2013).

The SCN is not special in having this loop; instead, it acts to transduce luminance information into synchronization of its own cells' clocks, and in turn clocks throughout the rest of the body, establishing an organismal "time zone." To this end, it has a number of special clock properties that separate it from most other tissues, including a robust and sustained rhythm even in the absence of exogenous timing cues, a susceptibility of its overall rhythm to phase and period changes by light, and a resistance of its overall rhythm to phase and period changes by non-photic cues (Abe et al, 2002; Buhr et al, 2010). The overall SCN network, rather than something intrinsic to its individual cells, predominantly underlies most of these properties.

The machinery required to carry out these functions is impressively intricate. Highlighting its [network] complexity, the SCN secretes literally hundreds of distinct neuropeptides derived from at least 24 prohormones and numerous other proteins (Southey et al., 2014), along with cytokines, small-molecule neurotransmitters like GABA and nitric oxide, and others. Many of these signals have well-understood circadian roles (reviewed in Slat et al., 2013). For example, vasoactive intestinal peptide (Vip) and gastrin releasing peptide (Grp) maintain synchrony of SCN cellular oscillators and behavioral rhythmicity, and entrain them to light (Piggins et al., 1995; Harmar et al., 2002; Colwell et al., 2003; Aton et al., 2005; Brown et al., 2005; Gamble et al., 2007; An et al., 2011; Maywood et al., 2011). Arginine vasopressin (Avp) also strengthens SCN and behavioral circadian rhythmicity, but unlike Vip and Grp, potentiated phase shifting in animals lacking its receptors suggests Avp signaling acts to buffer and restrain light entrainment of the central clock (Li et al., 2009; Maywood et al., 2011; Yamaguchi et al., 2013). Prokineticin-2 (Prok2) acts primarily as an output that couples the SCN to other brain regions (Cheng et al., 2002; Prosser et al., 2007). More recently, high-throughput peptidomic and circuit

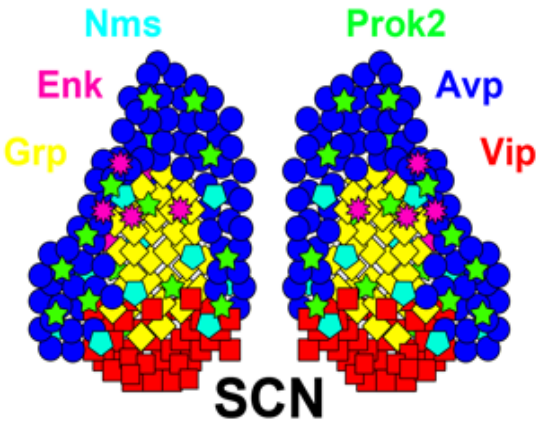

Figure 1.1: Neuron Diversity in the Adult SCN. A diagram of the adult SCN, showing a subset of its many neuropeptidergic populations. Neuropeptide colors are indicated by their names, positioned around the SCN. Note that many of these neuropeptides cross or exist outside of the classical core and shell SCN subdomains. Also note that many of these neurotransmitters are at least partially co-expressed, such as in Vip/Grp neurons, though the various probable combinations are not shown here for simplicity.

mapping approaches have identified novel SCN signals that play important parts in circadian physiology, such as integration of glutamatergic SCN input by the neuropeptide little SAAS and the as-yet-unidentified cue(s) secreted by neuromedin S-(+) neurons that are essential for SCN pacemaker function (Atkins et al., 2010: Lee et al., 2015). Although the SCN is classically thought of as having a ventrolateral core and dorsomedial shell subdomains (Abrahamson and Moore, 2001), many of its prominent neuropeptides do not respect those delineations (Figure 1.1; reviewed in Morin et al, 1992) , and co-expression of these signals adds yet more complexity to the picture (Albers et al, 1991; Lee et al, 2015; Okamura et al, 1986).

Neuropeptide expression is an instructive microcosm of SCN complexity, and one I will return to frequently throughout this thesis. However, other aspects of SCN anatomy and function, such as patterned expression of other classes of genes, the disposition of its afferents and efferents, and the temporal organization of molecular clock properties across multiple spatial axes, are just as complex (reviewed in Bedont and Blackshaw, 2015). Furthermore, these features are coordinated in tandem. For instance, vlSCNmain cells of the rat SCN consistently express rhythmic Vip and Grp, are light responsive, and are densely innervated by intrinsically photosensitive retinal ganglion cells (ipRGCs). In contrast, vlSCNmed cells express arrhythmic Vip alone, are light unresponsive, and receive little ipRGC innervations (Kawamoto et al, 2003). Coordination of such myriad features is very likely the rule, rather than the exception, across SCN cell types. How the developing SCN allows for both such variety and such consistent co-regulation of adult features during the region's development presents a

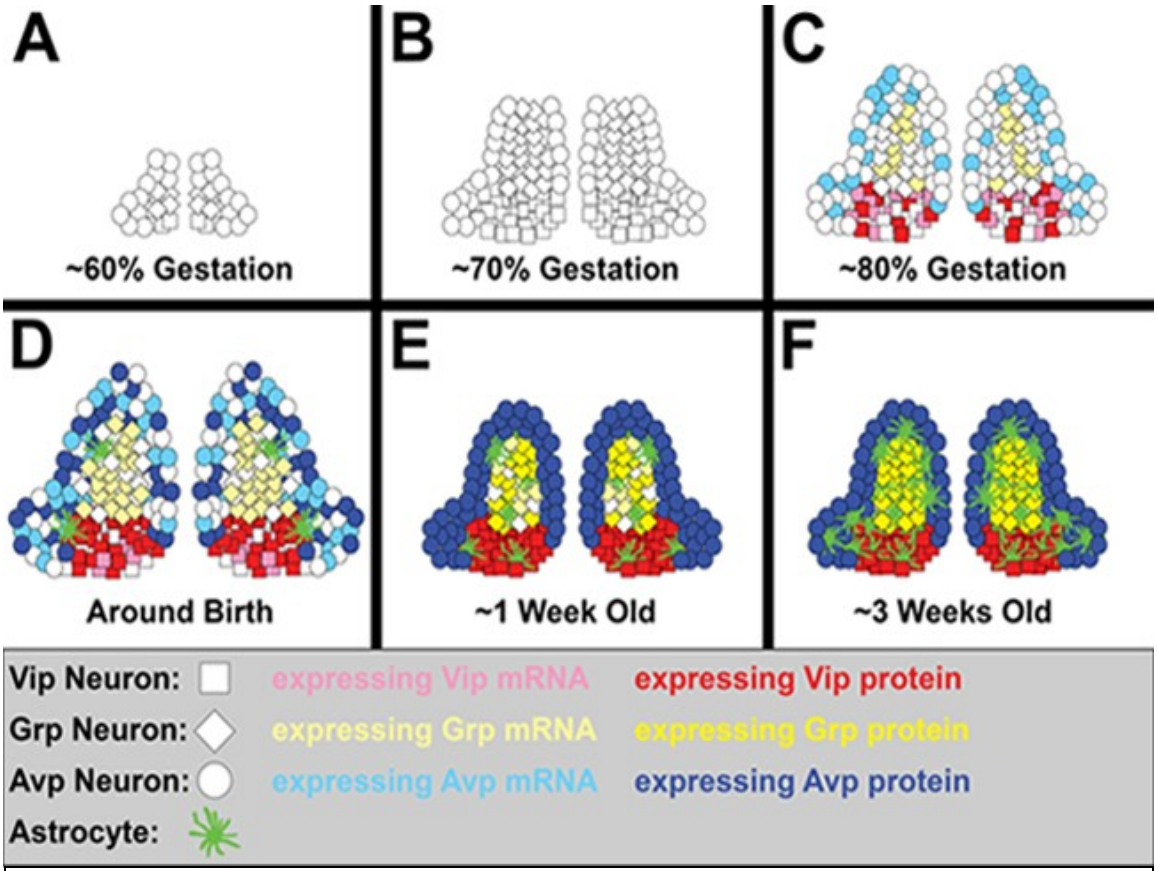

Figure 1.2: SCN neurogenesis and differentiation. A simplified diagram showing the development of Vip, Grp, and Avp neurons, as well as astrocytes, in the rodent SCN. While domain boundaries are depicted as relatively static here to aid in illustrating our points, they are actually quite dynamic over the course of development. **(A)** Early SCN neurogenesis begins at ~60% of gestation (hamster E9.5, mouse E12, and rat E13.5). **(B)** By ~70% of gestation (hamster E11, mouse E13.5, rat E15), most ventrolateral neurons have been produced, while dorsomedial neurogenesis is still in full swing. **(C)** The final major burst of SCN neurogenesis (including a number of ventrolateral neurons) occurs at ~80% of gestation (hamster E12.5, mouse E15, rat E17). Shortly thereafter, many SCN neuropeptide transcripts, but only Vip protein, are detectable (hamster E13, mouse E18-P0). **(D)** Shortly before and after birth, the first SCN astroglia appear (hamster E15, rat E20), Avp protein expression is detectable (P1), and SCN neuron number peaks (hamster P2). **(E)** By roughly a week into life, astrocyte number has jumped substantially (rat P3-P4), cell death brings neuron numbers down to adult levels (hamster P5, mouse P7, rat P6), and Grp protein expression is detectable (hamster P8). **(F)** By the end of the second major jump in astrocyte number (rat P20-25), the SCN is largely mature. At this stage, the fate of its neurons and its subdomain boundaries are relatively stable, though they may remain somewhat malleable under circadian challenge from the environment.

tantalizing biological puzzle, which I shall focus on for the remainder of this introduction.

1.2.2. Phenomenology of SCN Development

So far, much of the data speaking to cell fate decisions in the SCN comes in the form of correlative evidence from phenomenological studies, such as the relationship between date of neurogenesis during development and neuropeptide fate in the adult SCN. The bulk of SCN neurogenesis occurs between ~60–80% of gestation in rodents, at approximately E9.5-12.5 in hamster, E12-15 in mice, and E13.5-17 in rat (Figure 1.2 A-C; Altman and Bayer, 1978; Crossland and Uchwat, 1982; Davis et al., 1990; Antle et al., 2005; Kabrita and Davis, 2008). Studies in mouse and hamster suggest that genesis of vlSCN neurons consistently peaks earlier than dmSCN neurons in rodents, in contrast to the anteroposterior timing of SCN neurogenesis, which shows much greater species-dependent variation (Davis et al., 1990; Kabrita and Davis, 2008). Correspondingly, cell types enriched in hamster SCN core and central domains such as Vip, Grp, and calbindin (Calb1) are mostly born early, while Avp(+) neurons of the shell can be born at any time during the period of neurogenesis (Antle et al., 2005) (Figure 1.2 A–C). An interesting exception to this trend is a distinct subset of Vip and Calb1 neurons that are born at the end of rat SCN neurogenesis (Abizaid et al., 2004), likely corresponding to the final burst of vlSCN neurogenesis in hamsters (Figure 1.2 C-D; Davis et al., 1990). As in most brain regions, astrogliogenesis follows neurogenesis in the SCN, with the astrocyte marker glial fibrillary acidic protein (Gfap) first detectable shortly before birth, at E15 in hamsters and E20 in rats (Figure 1.2 D; Botchkina and Morin, 1995; Munekawa et al., 2000).

Many of these decisions are completed *in utero*, as the neurotransmitter fate(s) chosen by SCN neurons begin to become clear late in embryonic development. Many SCN neuropeptide mRNAs, including Vip, Avp, Grp, and Prok2, are first detectable by in situ hybridization between E18 and birth in mouse SCN, though generally in numbers lower than seen in adults, suggesting that not all SCN neurons are differentiated at this time (Figure 1.2 C; Shimogori et al., 2010; VanDunk et al., 2011; Bedont et al., 2014; Allen Brain Atlas). In contrast, SCN neuropeptide proteins first become detectable at more variable ages than do their mRNAs. In hamster SCN, Vip is present by E13 (only slightly earlier than Vip mRNA in mouse, adjusted for gestation), while Avp is present by P1, Grp is present by P8, and substance P (Sp) is present by P10 (Figure 1.2 C-E; Romero and Silver, 1990; Botchkina and Morin, 1995; Antle et al., 2005). The first major increase in rat SCN Gfap expression, indicating astrocytic maturation, also occurs during this time at ~P3-P4 (Figure 1.2 E; Munekawa et al., 2000).

That said, the final disposition of SCN subpopulations remains at least somewhat plastic post-natally. Cell death removes a substantial subset of SCN neurons over the course of early post-natal life, concurrent with the formation of a large percentage of SCN synapses (Figure 1.2 D; Ahern et al, 2013; Moore and Bernstein, 1989; Muller and Torrealba, 1998). Both domain boundaries and the morphology of individual cells also remain plastic during this early post-natal period, as they progress toward their fully differentiated states (Moore and Bernstein, 1989; Delville et al, 1994; Botchkina and Morin, 1995; Herzog et al, 2000; Antle et al, 2005). The SCN appears to reach a more-or-less adult state around weaning age, at which point astrocyte development as indicated by adult levels of Gfap expression is complete (Munekawa et al, 2000).

1.2.3 Mechanisms of SCN Development

Until very recently, the extracellular signals and cell-autonomous factors that guide this drawn-out developmental process were unclear. Beginning with extracellular signaling, the precise influence of early morphogens is largely speculative. For example, while Sonic hedgehog (Shh) from the basal plate is required for early SCN patterning and specification, much like the rest of the anterior hypothalamus, its down-regulation midway through SCN neurogenesis is suggestive but has no proven role in fate selection of SCN cell types (Shimogori et al, 2010; Alvarez-Bolado et al, 2012). Similarly, SCN progenitors are competent to respond to Wnt signaling via transient *Fzd5* expression, but what effect this may have on SCN development is even more poorly understood than Shh (VanDunk et al, 2011).

Moving a bit later in development, definitive proof exists for roles of monoamines and PSA-NCAM signaling in SCN fate selection. Rat pups exposed to a pharmacological inhibitor of synthesis for the SCN input serotonin (5HT) from E13-E21 have more Vip and possibly Avp neurons, and increased cellular expression levels of these neuropeptides, in the SCN; however, this effect does not occur if the pups are instead treated with the drug early in post-natal life (Ugrumov et al., 1994; Mirochnik et al., 2005). Paradoxically, similarly increased numbers of Vip and Avp neurons and neuropeptide levels in SCN were observed in monoamine oxidase A null mice, which have constitutively elevated levels of monoamine neurotransmitters including 5HT. Increases in neuropeptide expression levels, but not cell number, could be reversed by 5HT or norepinephrine inhibitors administered post-natally (Vacher et al., 2003). One possible rationalization of these results is that embryonic inhibition of 5HT synthesis

causes homeostatic up-regulation in other monoamine pathways to compensate. In another set of studies, mice selectively deficient for PSA-NCAM expressed in the dorsal SCN have three times the usual number of Vip neurons, in an expanded vlSCN (Shen et al., 1997, 1999). Thus, both PSA-NCAM and monoamine neurotransmitters are most likely regulating the differentiation of SCN neuropeptide lineages. However, another more intriguing possibility is that the overall fate of SCN neurons may remain plastic during their maturation, and can be manipulated by these extracellular cues.

Whichever is true, subpopulations of SCN neurons remain dependent on external signaling for maintenance and maturation of their fate as development progresses. For instance, Fgf8 signaling is required for SCN Avp expression, likely due to a role in maturation of these cells as it is elsewhere in the hypothalamus (Brooks et al, 2010; Tsai et al, 2011). Furthermore, though the evidence is indirect, it is likely that SCN neurotransmitters themselves shape fate selection, maintenance, and maturation in later-born populations. The earliest synapses form in rat SCN at E19, shortly after Vip first appears in the E13 hamster SCN adjusted for gestation (Moore and Bernstein, 1989). Hamster Vip neurons already begin to extend axons as early as E15, though the scarcity of synapses suggests that any signaling they engage in during neonatal life is likely paracrine (Botchkina and Morin, 1995). This situation changes rapidly with increasing synapse formation between P2-P6, shortly after Avp expression is first detected, followed shortly thereafter by another increase that drives synapse density to adult levels by P10 (Moore and Bernstein, 1989). This phenomenon may be related to the exclusion of dying cells from clusters formed by healthy cells in early post-natal life, when most SCN cell

death occurs, suggesting a role in extracellular signaling in regulating apoptosis (Moore and Bernstein, 1989).

Thus, while the picture for the role of extracellular factors in SCN fate selection is decidedly fragmented, a number of actors and potential actors have been identified. In contrast, prior to the publication of my work on Lhx1, the only know cell-autonomous transcription factors involved in SCN development were involved in very early specification of the entire nucleus, reflected in an early-onset and sometimes transient expression pattern in the SCN (Figure 1.3). For instance, Lhx2−/− mice fail to down-regulate dlAH markers such as Sim1 and Otp and up-regulate early vAH gene expression such as Vax1 and Lhx1 by embryonic day (E) 12.5, when AH subdivisions are normally clearly defined (Roy et al., 2013). These mice would almost certainly fail to specify an SCN (Figure 1.3). However, Lhx2 is expressed in cells surrounding the SCN by birth, rather than in the SCN proper, suggesting it may play more of a role in early specification of dlAH and vAH identity than in promoting SCN specification per se (VanDunk et al., 2011).

Unlike Lhx2 and many other early AH and vAH factors that are down-regulated in SCN later in development, Six3 expression remains expressed in the vAH throughout the lifespan, and is required cell-autonomously for initial SCN specification (Figure 1.3; Shimogori et al., 2010; VanDunk et al., 2011). Its homolog Six6 has a similar, although more restricted, enduring vAH expression pattern, and is also required for initial SCN specification (Figure 1.3; Shimogori et al., 2010; Clark et al., 2013). In this context, the identification of Lhx1 as one of the earliest markers of the emerging SCN lineage at mouse E11.5 suggested it as a promising topic for my thesis to focus upon. While it

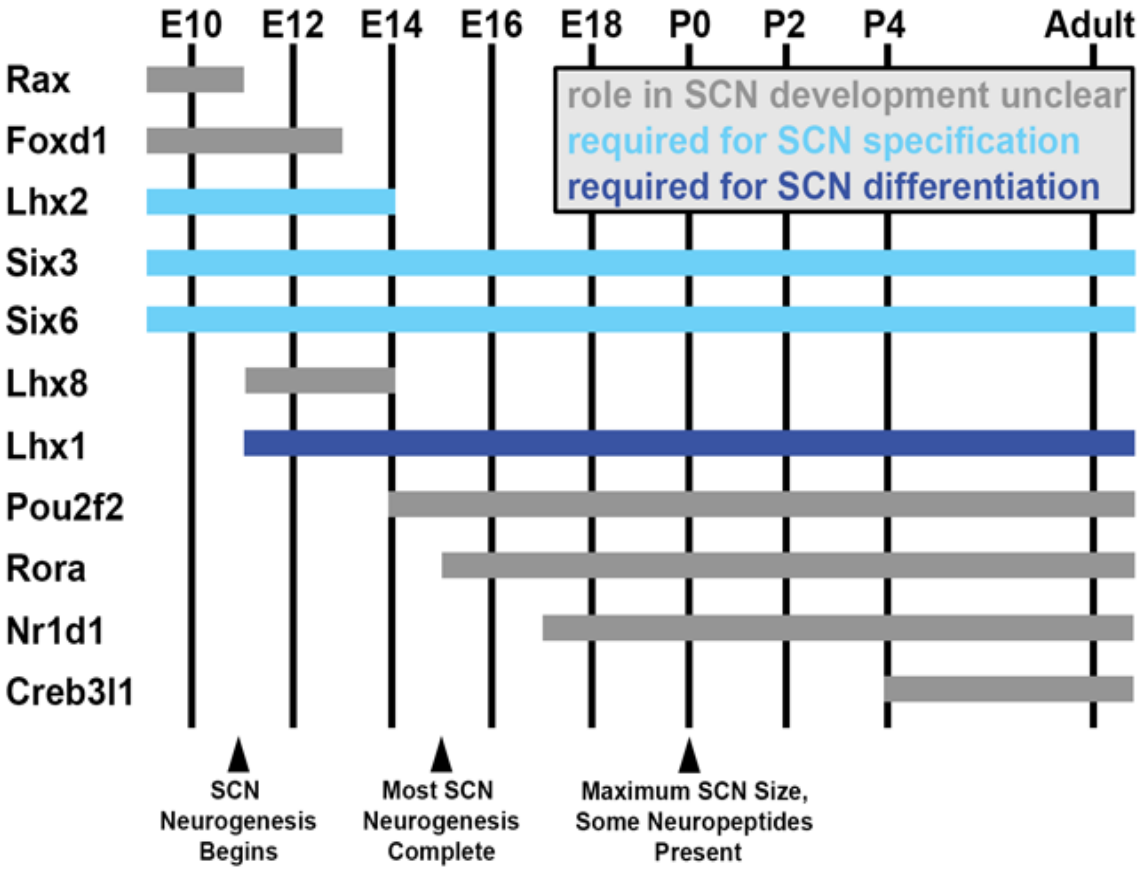

Figure 1.3: SCN transcription factor expression during development. Estimated ages of expression for a subset of hypothalamus- and SCN-enriched transcription factors in the developing mouse SCN between embryonic day (E) 10 and adulthood, selected based on interesting expression patterns and/or known developmental functions (indicated by bar color). Note that many general hypothalamic transcription factors (expressed prior to E10) are downregulated as the transcriptional network controlling SCN development ramps up. Not shown in this figure, other transcription factors expressed throughout the SCN during its development in turn become progressively compartmentalized to specific subdomains as the SCN matures (ex: Lhx1, Rorα).

was possible that it would merely be required for SCN specification, like the other factors identified previously, we hoped to instead identify the first factor involved in the differentiation and fate selection of SCN lineages (Figure 1.3; Shimogori et al, 2010; VanDunk et al, 2011). And, indeed, this was what came to pass.

Chapter 2: Lhx1 Controls SCN Terminal Differentiation

Large parts of this chapter are direct excerpts and/or paraphrased passages from Bedont et al, 2014.

2.1 Introduction

Unlike Six3, Six6, and Lhx2, hypothalamic expression of other transcription factors is restricted to the SCN during development, the earliest of which is LIM homeodomain transcription factor 1 (Lhx1) (Shimogori et al., 2010 and VanDunk et al., 2011). Lhx1 guides differentiation of other neural subtypes outside the hypothalamus, including cerebellar Purkinje cells (Zhao et al., 2007) and hindbrain reticulospinal neurons (Cepeda-Nieto et al., 2005). Intriguingly, it also dictates neuropeptide fate of specific cell subpopulations during spinal cord development (Bröhl et al., 2008). Given this data, we hoped to identify a role for Lhx1 in guiding SCN differentiation.

2.2 Materials and Methods

Animals and Housing

Six3-Cre;Lhx1$^{lox/lox}$ and control *Lhx1*$^{lox/lox}$ mice, along with *Vip*$^{-/-}$ and control *Vip*$^{+/+}$ mice, were used, with the following exceptions: *Six3-Cre;Lhx1*$^{lox/lox}$*;Opn4*$^{lacZ/+}$ and *Lhx1*$^{lox/lox}$*;Opn4*$^{lacZ/+}$ mice for X-gal staining, *Six3-Cre;Lhx1*$^{lox/lox}$*; Per2*$^{luc/+}$ and *Lhx1*$^{lox/lox}$*;Per2*$^{luc/+}$ mice for luciferase imaging, and *Six3-Cre;ROSA26::YFP* mice for Cre mapping. Genetically modified mice were provided by Y. Furuta (*Six3-Cre*), R. Behringer (*Lhx1*$^{lox/lox}$), and Jackson Laboratories (*Per2::luc* and *Vip*$^{-/-}$). Behavioral studies used males; other experiments used both sexes. Except where otherwise noted, mice were on a 15 hr:9 hr light:dark cycle. All mice were mixed C57BL6/Sv129 background [excepting *Vip*$^{-/-}$ mice, which are pure C57BL6]. All controls were

littermates. All procedures and care were approved by Johns Hopkins Institutional Animal Care and Use Committee, in line with National Institutes of Health guidelines for experimental animals.

Genotyping

Transnetyx conducted most genotyping using proprietary methods. Some floxed Lhx1 alleles were genotyped as described previously (Kwan and Behringer, 2002), and some Cre was detected by presence of a ~300 bp band amplified using primers 5′-TTCCCGCAGAACCTGAAGAT-3′ and 5′-CCCCAGAAATGCCAGATTAC-3′.

RNA Sequencing

Whole brains were freshly dissected over the course of an afternoon from adult *Six3-Cre;Lhx1*$^{lox/lox}$ and *Lhx1*$^{lox/lox}$ mice and placed ventral side up in a stainless steel brain matrix (Kent Scientific) pre-chilled on ice. Under a Leica MZ95 dissecting microscope, the optic nerves were cut away and razor blades were positioned coronally on either side of the SCN, using the optic chiasm as a landmark. The razor blades were pressed through the brain in one swift, smooth motion and the coronal surface of the brain anterior and posterior to the cuts was examined, to ensure that the entire anteroposterior breadth of the SCN was captured. The optic chiasm was gently removed from the resulting 1 mm thick brain slice with Bioscissors (Oban Precision Instruments) and forceps, and samples of SCN were taken using a 1 mm diameter stainless steel sample corer (Fine Science Tools) and deposited with forceps directly into Qiazol chilled on ice. Five SCN punches were pooled for each of three biological replicates, one male and two female.

As soon as all dissections were completed for a given biological replicate, all tissues were homogenized in Qiazol using a Kimble Kontes motorized pellet pestle, and

RNA was extracted using an RNeasy lipid tissue mini kit (Qiagen) per manufacturer instructions. RNA integrity was validated by Nanodrop (Thermo Scientific) and electrophoresis. A cDNA library was then generated from the collected RNA using a TruSeq Stranded Total RNA kit (Illumina). Libraries were barcoded and multiplexed 2-3 per lane, and sequenced to a paired-end read depth of 100 cycles. Fastq files were aligned using TopHat and fold changes were calculated using Cufflinks on Galaxy (Goecks et al, 2010; Trapnell et al, 2012). Cutoffs of at least 2X fold change and higher FPKM>1 were applied, and peaks from all qualifying hits were inspected visually using the UCSC brower to validate the Cufflinks-generated fold change. We also manually pulled out a number of genes of interest that were triaged by our cutoffs, and visually inspected them on the UCSC browser. Hits that passed this three-part validation process were considered for post-hoc ISH analysis.

Tissue Preparation for Histology

Brains were dissected, fresh frozen in OCT (Tissue-Tek) at the desired age, and stored at −80°C. Each experimental/control pair was collected in the same session. 25 μm serial sections were cut on a Leica CM3050-S cryostat, thaw mounted on Superfrost Plus slides (Fisher), and stored at −80°C. Five adjacent slide sets were prepared for ISH; two were prepared for IHC and TUNEL.

In Situ Hybridization (ISH)

Probes were selected and tissue processed as previously described (Shimogori et al., 2010).

Immunohistochemistry (IHC)

Slides were fixed in 4% paraformaldehyde in 1× PBS, blocked in Superblock (Thermo Scientific), and then incubated overnight at 4°C in 1:200 monoclonal mouse immunoglobulin G (IgG) 2b anti-human-HuC/D (Invitrogen) or 1:500 polyclonal rabbit IgG anti-GFP (Molecular Probes) in PBS (5% horse serum, 0.16% Triton X-100 in 1X PBS). Slides were then incubated in 1:500 goat anti-mouse Alexa 568 IgG (Molecular Probes) or 1:500 donkey anti-rabbit Alexa 488 IgG (Molecular Probes), DAPI stained, and coverslipped with Gelvatol.

TUNEL Cell Death Assay

Slides were processed with TMR Red In Situ Cell Death Kit (Roche) following the manufacturer's instructions for cryopreserved tissue.

MOPAT Bioinformatic Analysis

The Lhx1 transcription factor binding site position weight matrix was downloaded from the Bulyk PDM Database (http://the_brain.bwh.harvard.edu/pbms/webworks2/explore.php). Proximal enhancer regions (2 kb upstream and 1kb downstream of transcription start site) were extracted from annotated reference genes, and only sequences conserved between mouse and human genomes were considered. We identified Lhx1 binding sites with motif pair tree (MOPAT) software (Hu et al., 2008), with 0.0001 as the p value cutoff defining positive hits.

2.3 Results

2.3.1 Validation of Six3-Cre;Lhx1$^{lox/lox}$ Targeting Strategy

Because conventional *Lhx1* null mice lack anterior neural structures (Shawlot and Behringer, 1995), we used an intersectional approach to more specifically delete Lhx1 in the developing anterior hypothalamus by crossing a conditional allele to transgenic *Six3*-

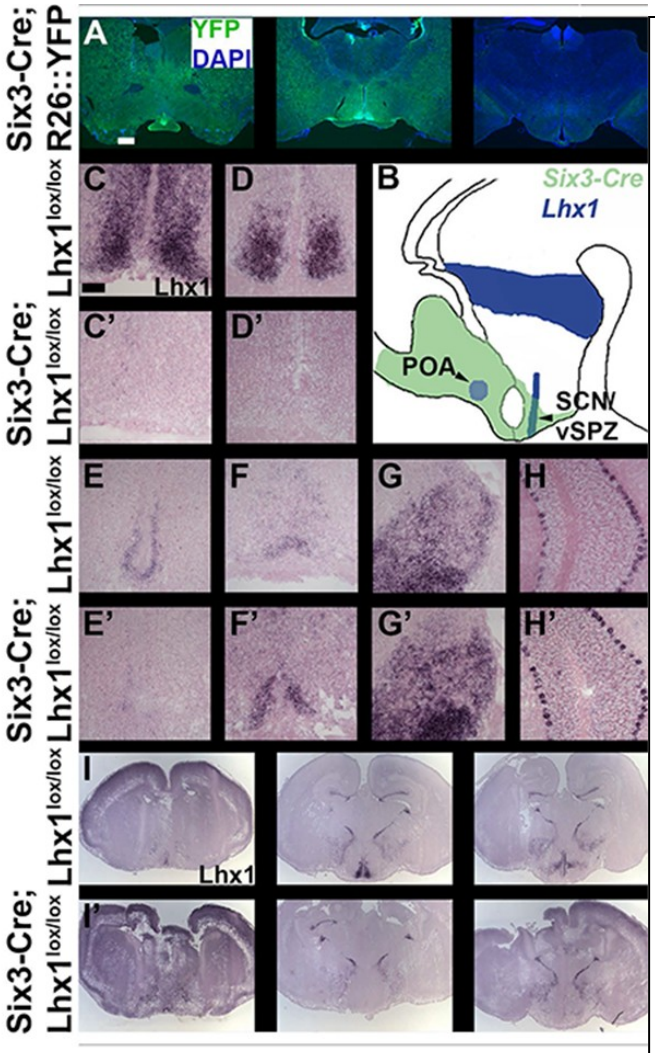

Figure 2.1: Selective *Lhx1* deletion in the anterior hypothalamus by the *Six3-Cre* driver. (A) α-YFP IHC (green) and DAPI stain (blue) in *Six3-Cre;ROSA26::YFP* brains showed robust Cre activity in SCN, vSPZ, and POA and modest activity throughout AH, but little to none in more posterior regions. Coronal planes arranged anterior (left) to posterior (right). Scale bar = 500um. **(B)** Sagittal schematic of E12.5 Six3-Cre activity and *Lhx1* expression. **(C-H)** Coronal high magnification ISH of *Lhx1* expression in $Lhx1^{lox/lox}$ (C-H) and *Six3-Cre;*$Lhx1^{lox/lox}$ (C'-H') mice in P0 SCN (C,C') and adult SCN (D,D'), vSPZ (E,E'), POA (F,F'), IGL (G,G'), and cerebellum (H,H'). Scale bar = 100um. **(I)** Coronal low magnification ISH of *Lhx1* expression in $Lhx1^{lox/lox}$ (top) and *Six3-Cre;*$Lhx1^{lox/lox}$ (bottom) mouse brain including POA (left), SCN (middle), and SPZ (right).

Cre mice (Furuta et al., 2000; Kwan and Behringer, 2002). As previously reported, *Six3-Cre* activity was more spatially restricted than native Six3 expression (Furuta et al., 2000). *Six3-Cre; ROSA26::YFP* mice had robust Cre activity in the ventral telencephalon and ventral anterior hypothalamus, including the SCN and subparaventricular zone (SPZ). However, *Six3-*

Cre;ROSA26::YFP mice lacked Cre activity in more posterior regions that express Lhx1 during embryonic development, such as the intergeniculate leaflet (IGL), dorsomedial hypothalamus, and mamillary nucleus (Figure 2.1 A-B). Lhx1 in situ hybridization (ISH) revealed that *Six3-Cre;Lhx1*$^{lox/lox}$ mice reliably and specifically lost *Lhx1* expression in the ventral anterior hypothalamus, including the SCN and SPZ (Figure 2.1 C-E,I). Although transient Lhx1 expression in anterior hypothalamic nucleus and anterior lateral hypothalamus were also lost at postnatal day 0 (P0) (Figure 2.1 I), neither region has any established circadian function. Lhx1 was normally expressed in more posterior regions important for circadian rhythmicity and motor output (e.g., IGL, cerebellum) as well as the medial preoptic area (Figure 2.1 F-H).

2.3.2 RNA Sequencing of Six3-Cre;Lhx1$^{lox/lox}$ SCN Gene Expression

In order to conduct an unbiased analysis of SCN-enriched gene expression driven by Lhx1, we conducted RNA sequencing on SCN tissue punches. Strikingly, a large number of transcripts encoding neuropeptides and proteins that transduce or modify post-synaptic signals of neuropeptides were down-regulated in our dataset. These included the neuropeptides Vip, Nms, Grp, Prok2, and Vgf; the neuropeptide GPCRs Npy6r, Avpr1a, and Grpr; Ras-family GTPases Rasl11b and Rasa4; the cAMP-producer Adcy3; and several other regulators of GPCR and MAPK signaling (Table 2.1).

.However, we noted that two neuropeptides (Avp and Penk) that we had previously shown are down in *Six3-Cre;Lhx1*$^{lox/lox}$ mutants (Bedont et al, 2014) did not reach the fold-change cutoffs applied to our RNA sequencing data. This was likely due to contamination for brain regions in close proximity to the SCN, which express these factors at substantially higher levels than the SCN itself.

UCSC ID	Gene Symbol	Function	Fold Change
uc008euv.1	Npy6r	neuropeptide GPCR	-9.21
uc007egk.1	Vip	neuropeptide	-5.86
uc007atb.1	Nms	neuropeptide	-4.12
uc009eir.1	Styk1	receptor tyrosine kinase, may regulate MAPK signaling	-2.85
uc008xtj.1	Rasl11b	ras-like GTPase	-2.79
uc008ffk.1	Grp	neuropeptide	-2.75
uc009dbu.1	Prok2	neuropeptide	-2.69
uc007dae.2	Rgs16	GTPase activator, modulates cAMP production	-2.56
uc008kxf.1	Creb3l1	transcription factor that regulates Avp neuropeptide levels	-2.18
uc009lks.1	Dusp4	protein phosphatase, regulates MAPK signaling	-2.07
uc007xyj.1	Ppp1r1a	protein phosphatase-1 inhibitor, modulates cAMP production	-2.04
uc009abn.2	Serpine1	regulator of protease and GPCR activity	-2.01
uc008hnh.1	Avpi1	marker of Avp signaling	-1.86
uc012dxj.1	Kit	receptor tyrosine kinase	-1.76
uc009abl.1	Vgf	neuropeptide	-1.74
uc008zzv.1	Rasa4	ras family GTPase	-1.69
uc007hge.1	Avpr1a	neuropeptide GPCR	-1.6
uc009uuu.1	Grpr	neuropeptide GPCR	-1.55
uc007mxl.2	Adcy3	signal transduction via cAMP synthesis	-1.34

Table 2.1 RNAseq hits: SCN-enriched genes down-regulated after local Lhx1 deletion. Genes with fold-change of -2.0 or greater were screened in an unbiased manner, in accordance with our cutoffs for fold change and higher FPKM. Genes with fold-change of less than -2.0 were checked manually on UCSC due to their functional relationships with other genes that reached our cutoffs.

2.3.3 In Situ Hybridization Analysis of Six3-Cre;Lhx1$^{lox/lox}$ SCN Gene Expression

Prior to our RNA sequencing data, we had examined neuropeptide expression in *Six3-Cre;Lhx1*$^{lox/lox}$ and *Lhx1*$^{lox/lox}$ control SCN by ISH. Neuropeptides implicated in circadian function were downregulated (Figure 2.2 A–G), including Vip, Prok2, Grp, Avp, Enk, and Nms ($p < 0.05$ for all except Grp, and $p < 0.005$ for Grp). Downregulation was not observed in other brain regions (Figure 2.2 A–F). SCN neuropeptide loss was not

caused by the Cre driver alone, because *Six3-Cre;Lhx1*$^{+/+}$ mice had normal expression of Vip, Grp, Avp, and Lhx1 (data not shown).

Importantly, other SCN markers were largely unaffected by Lhx1 deletion (Figures 2.3, 2.4). GABAergic markers such as Gad67, Calb1, and Calb2 were retained

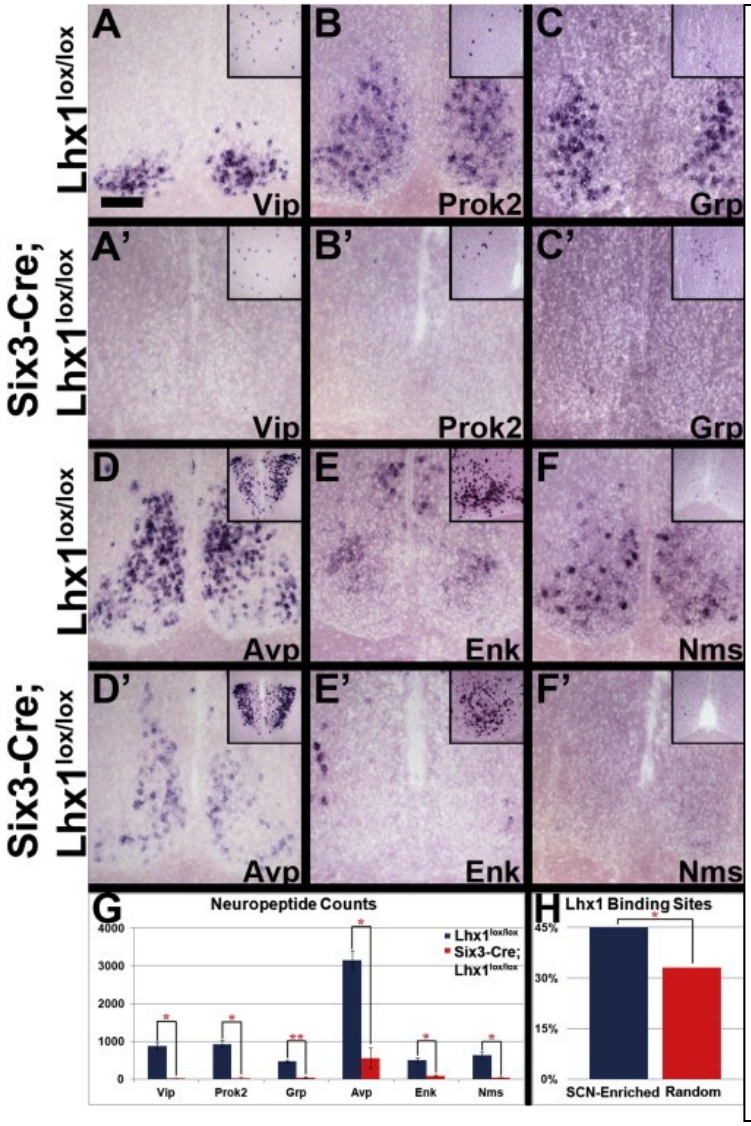

Figure 2.2: Lhx1 effects on SCN neuropeptides. **(A–F′)** ISH of SCN from adult *Lhx1*$^{lox/lox}$ control (A–F) and *Six3-Cre;Lhx1*$^{lox/lox}$ mutant (A′–F′) mice for Vip (A, A′), Prok2 (B, B′), Grp (C, C′), Avp (D, D′), Enk (E, E′), and Nms (F, F′). Insets show other unaffected brain regions for comparison. Scale bar = 100 μm. **(G)** Mutants had fewer labeled SCN cells than controls (n = 3, paired two-tailed t tests, $*p < 0.05$, $**p < 0.01$; graph depicts mean ± SEM). **(H)** MOPAT bioinformatic analysis showed more putative Lhx1-binding sites in enhancers of an SCN-enriched gene pool compared to a randomly selected pool (binomial distribution, $*p < 0.05$).

(Figures 2.3 A-C), as were SCN markers first expressed prior to induction of circadian neuropeptides during development, such as Vipr2, Id4, Arx, Dlx2, Nr1d1, and Rorb (Figures 2.3D and 2.4 A-E). Neuropeptides broadly expressed in the anterior hypothalamus were also mostly preserved in *Six3-Cre;Lhx1*$^{lox/lox}$ SCN, including Sst, Agt,

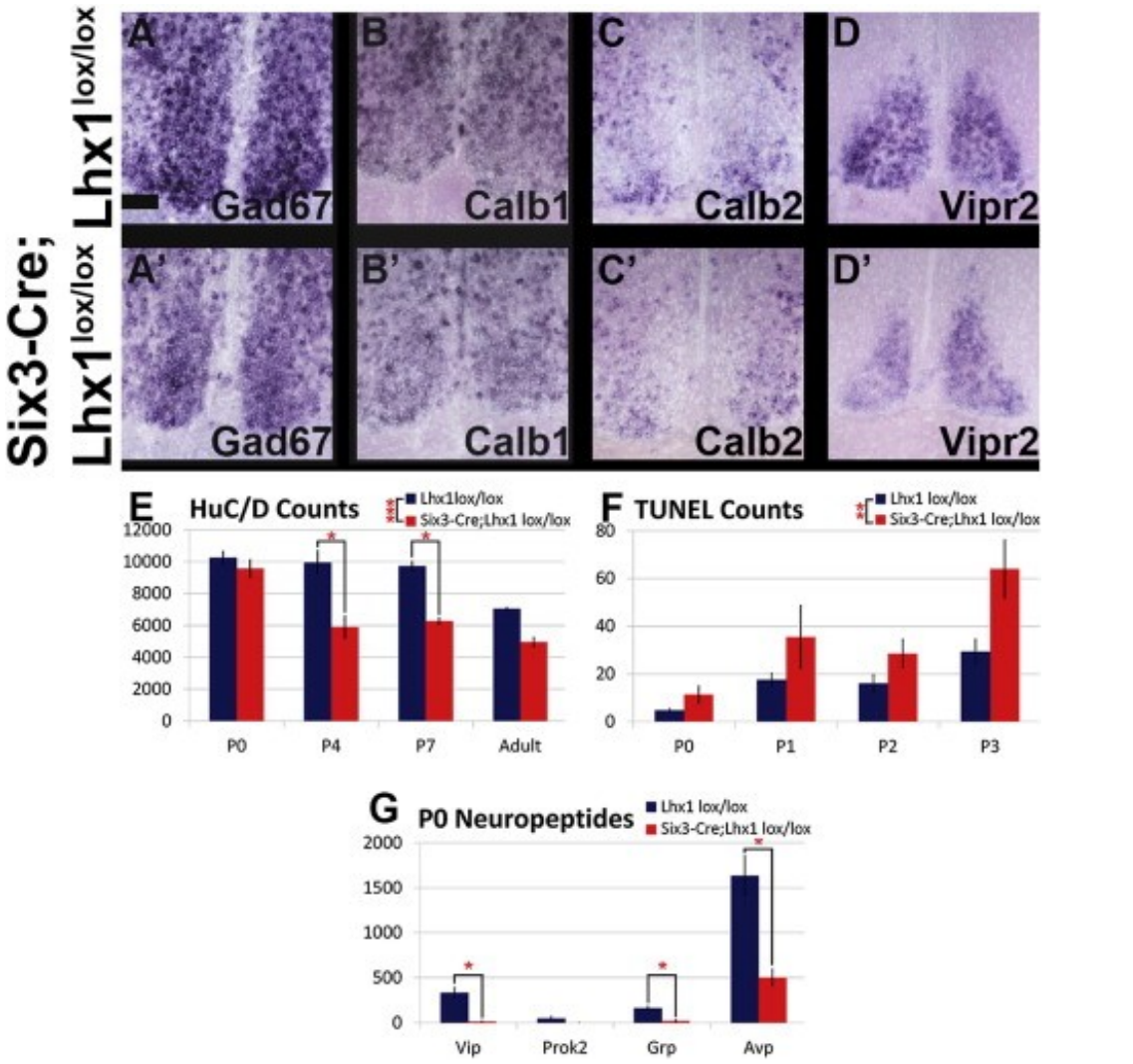

Figure 2.3: SCN regional identity is preserved in *Six3-Cre;Lhx1*$^{lox/lox}$ mice, but cell death is elevated in neonatal SCN. (A–D) ISH of SCN from *Lhx1*$^{lox/lox}$ control (A–D) and *Six3-Cre;Lhx1*$^{lox/lox}$ adult mutant (A′–D′) mice for Gad67 (A, A′), Calb1 (B, B′), Calb2 (C, C′), and Vipr2 (D, D′). **(E)** Mutants had fewer SCN neurons than controls at P4 and P7 (n = 3, 3, 3, 3, ANOVA and Tukey post hoc tests, $*p < 0.05$, $***p < 0.0005$; graph depicts mean ± SEM). Mutant SCN neuron number in adults was significantly lower than controls when initially analyzed on its own by t test ($p < 0.05$) but fell just short of significance in the context of the time course ($p = 0.07$). **(F)** Mutants had increased SCN cell death in the aggregate period between P0 and P3 compared to controls, but the age(s) within this range with elevated cell death could not be pinned down (n = 3, 4, 4, 3, ANOVA with post hoc Tukey tests, $**p < 0.005$; graph depicts mean ± SEM). **(G)** Mutants had fewer Vip, Grp, and Avp, but not Prok2, expressing SCN cells than controls at P0 (n = 3, 3, 3, 3, paired two-tailed t tests, $*p < 0.05$; graph depicts mean ± SEM).

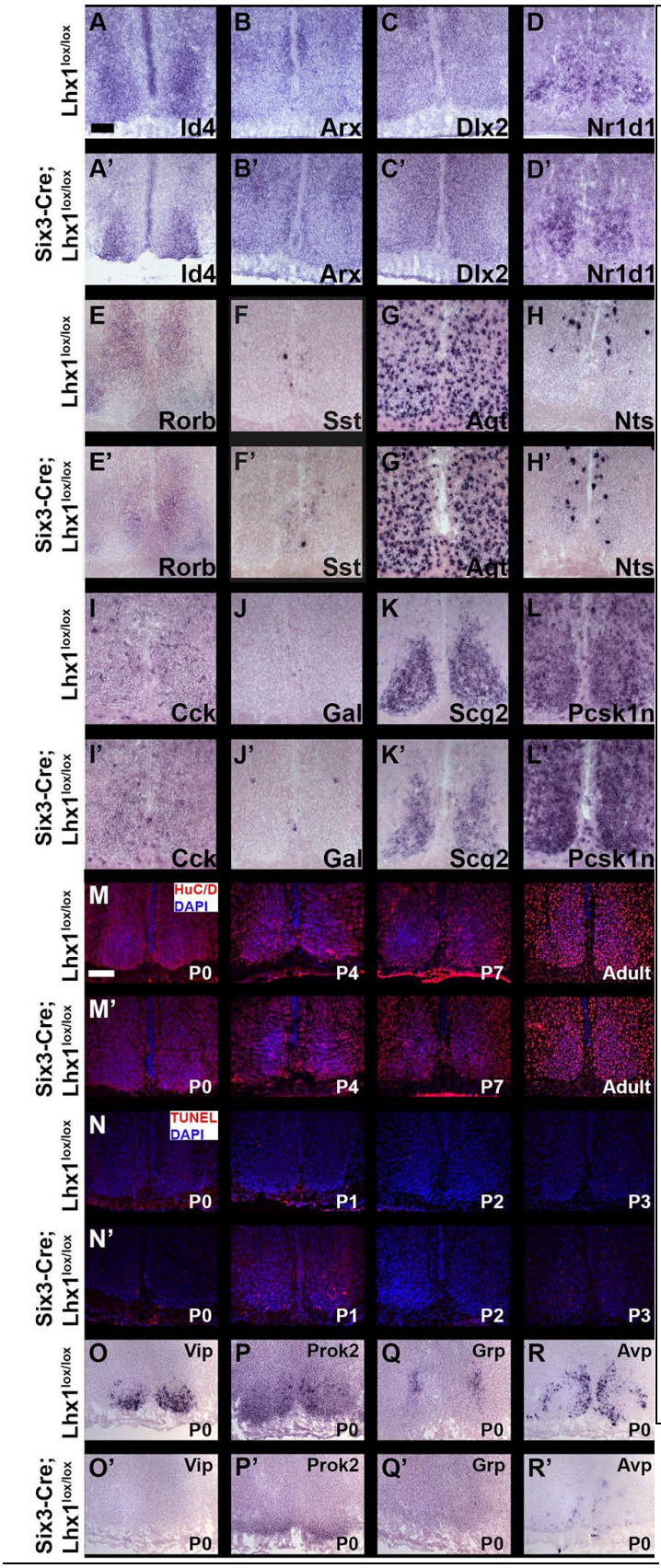

Figure 2.4: SCN regional differentiation occurs normally in *Six3-Cre;Lhx1*$^{lox/lox}$ mice, and loss of neuropeptidergic markers is not due to selective apoptosis in neonatal SCN. **(A-L)** ISH of SCN from *Lhx1*$^{lox/lox}$ control (A-L) and *Six3-Cre;Lhx1*$^{lox/lox}$ mutant (A'-L') mice for Id4 (A,A'), Arx (B,B'), Dlx2 (C,C'), Nr1d1 (D,D'), Rorb (E,E'), Sst (F,F'), Agt (G,G'), Nts (H,H'), Cck (I,I'), Gal (J,J'), Scg2 (K,K'), and Pcsk1n (L,L'). Adult SCN was used for all ISHs except A-C, which were P0. **(M)** Pan-neuronal α-HuC/D IHC (red) and DAPI stain (blue) of SCN from (left to right) P0, P4, P7, and adult *Lhx1*$^{lox/lox}$ control (M) and *Six3-Cre;Lhx1*$^{lox/lox}$ mutant (M') mice. Scale bar = 100um. **(N)** TUNEL stain (red) and DAPI stain (blue) of SCN from (left to right) P0, P1, P2, and P3 *Lhx1*$^{lox/lox}$ control (N) and *Six3-Cre;Lhx1*$^{lox/lox}$ mutant (N') mice. **(O-R)** ISH of SCN from P0 *Lhx1*$^{lox/lox}$ control (O-R) and *Six3-Cre;Lhx1*$^{lox/lox}$ mutant (O'-R') mice for Vip (O,O'), Prok2 (P,P'), Grp (Q,Q'), and Avp (R,R').

Nts, Cck, Gal, and Scg2 (Figure 2.4 F-K). Expression of Pcsk1n, required for proteolytic processing of many neuropeptide precursors, is also preserved (Figure 2.4L). Importantly, most markers normally restricted to specific SCN subdomains showed similar compartmentalization in mutants. For instance, Calb2 localized to ventral core, Rorb localized to shell, and Vipr2 expression remained weak in the center of the SCN (Figures 2.3 C-D and 2.4 E). Although ISH validation of our RNA sequencing screen is ongoing, most hits we have examined thus far appear to be confirmed.

2.3.4 Terminal Differentiation vs. Cell Death Defects in Six3-Cre;Lhx1$^{lox/lox}$ SCN

Pan-SCN ISH markers showed that *Six3-Cre;Lhx1$^{lox/lox}$* SCN was smaller than controls; therefore, we performed immunohistochemistry (IHC) for the pan-neuronal marker HuC/D and found that SCN neuron number was significantly reduced in *Six3-Cre;Lhx1$^{lox/lox}$* adults ($p<0.05$). To determine when neuron loss occurred in *Six3-Cre;Lhx1$^{lox/lox}$* SCN, we conducted HuC/D IHC at multiple developmental time points (Figures 2.3 E and 2.4 M). There were main effects of both genotype and age ($p<0.0005$) and significant interaction ($p<0.05$). SCN neuron number was normal at P0 in *Six3-Cre;Lhx1$^{lox/lox}$* mice ($p = 0.95$), but significantly fewer SCN neurons were present by P4 in *Six3-Cre;Lhx1$^{lox/lox}$* SCN compared to controls ($p<0.0005$) (Figures 2.3 E and 2.4 M). No further loss of neurons was observed in *Six3-Cre;Lhx1$^{lox/lox}$* SCN after P4, although neuron number continued to decrease gradually in control SCN into adulthood ($p<0.05$); this dropped the previously noted genotype difference in adult neuron number slightly below significance ($p=0.07$) in the context of the time course.

To examine whether decreased neuron number between P0 and P4 in *Lhx1*-deficient SCN resulted from increased developmental apoptosis, we conducted TUNEL experiments in P0–P3 SCN. A main effect of genotype ($p < 0.005$) indicated an aggregate increase in TUNEL-positive cells across the time course in *Six3-Cre;Lhx1*$^{lox/lox}$ SCN, although no individual time points were significant (Figures 2.3 F and 2.4 N). There was also a main effect of age ($p < 0.0005$) but no interaction ($p = 0.30$).

Given the prominence of neuropeptide signaling in the group of SCN-enriched genes lost after *Lhx1* deletion, we focused on a subset of down-regulated neuropeptides to assess whether gene expression changes were primarily a function of a terminal differentiation defect or cell death. To assess this, we measured neuropeptide expression by ISH at P0, when *Six3-Cre;Lhx1*$^{lox/lox}$ SCN neuron number is normal (Figures 2.3 G and 2.4 O-R). Vip, Avp, and Grp were already profoundly downregulated in mutant SCN, indicating that loss of neuropeptide gene expression precedes neuron loss (all $p < 0.05$; Figure 2.3 G). Prok2 expression was very low and variable in controls, making comparison with mutants uninterpretable (Figure 2.3 G). We did not detect Enk or Nms in control or mutant SCN by ISH at P0 (data not shown).

2.3.5 Mechanisms Underlying Lhx1 Control of SCN Gene Expression

We then conducted in silico MOPAT analysis to determine whether Lhx1 might directly regulate expression of SCN-enriched neuropeptides. A greater proportion of evolutionarily conserved predicted Lhx1 consensus binding sites were present within proximal regulatory regions of SCN-enriched genes relative to randomly selected genes (Figure 2.2 H). SCN-enriched genes bearing putative Lhx1 binding sites included the three neuropeptide genes with the greatest percent reduction in *Six3-Cre;Lhx1*$^{lox/lox}$ mice

(Vip, Prok2, and Nms) as well as Enk, which was not included in our initial analysis (Figures 2.2 G-H; Table 2.2). Shortly after our publication of this bioinformatic data, luciferase assays conducted by others further supported a role for Lhx1 in directly regulating expression of *Vip* (Hatori et al, 2014).

On the other hand, considering the loss of *Avp* known to occur in *Vipr2*$^{-/-}$ mice (Harmar et al, 2002), we were curious whether the loss of *Avp* in *Six3-Cre;Lhx1*$^{lox/lox}$ SCN was entirely due to the direct loss of Vip after *Lhx1* deletion, or whether multiple effectors are at work. To test this, we conducted ISH studies in *Vip*$^{-/-}$ mice, and found that the magnitude of *Avp* (and somewhat surprisingly, *Prok2*) neuron loss appeared quite similar to losses observed in *Six3-Cre;Lhx1*$^{lox/lox}$ SCN (Figure 2.5 A-B). In contrast, we found that the number of Grp and Nms neurons in *Vip*$^{-/-}$ SCN appeared similar to controls (Figure 2.5 C-D).

1810009M01Rik	Cacna1g	**Ephb1**	Lhx1	**Pcdh11x**	Rasa4	Setd6	**Trip10**
2310079N02Rik	**Calcr**	**Fhl1**	**Lhx8**	Pde5a	Rasd1	**Slc2a13**	Trp53i11
Adck4	Ccdc109b	**Flrt3**	**Magel2**	**Pde7b**	Rasl11b	**Slc39a6**	Vgf
Adcy3	Cdh13	Gpr56	Myo10	Per1	**Rftn1**	Slc6a11	**Vip**
Avp	Creb3l1	Grp	**Myt1**	Per2	Rgs16	**Snx25**	Vipr2
Avpr1a	**Ctf1**	**Grpr**	**Nms**	Per3	**Rgs4**	Spon1	**Ysk4**
B3gat2	D130067I03Rik	Id4	**Nnat**	Pik3r3	**Rora**	**Stk32a**	**Zfp462**
B630019K06Rik	**Dlk1**	**Igfbp5**	Nov	**Plc14**	**Rorb**	Syt10	**Zic1**
BC022623	**Drd1a**	**Iqsec3**	Nr1d1	Plekhg5	Rps6ka2	Tle4	Zim1
Bmal1	Dusp4	Itgb8	Nr1d2	**Prok2**	Sat1	Tnfrsf191	
Btg1	**Ednrb**	**Kcnk13**	Nxn	Prokr2	Sema6d	**Tnrc4**	

Table 2.2: Putative Lhx1-binding sites in SCN-enriched pool. All genes selected for the SCN-enriched pool are listed. Genes with putative Lhx1 binding sites are highlighted in red. Down-regulated neuropeptides with putative Lhx1 binding sites are highlighted in blue.

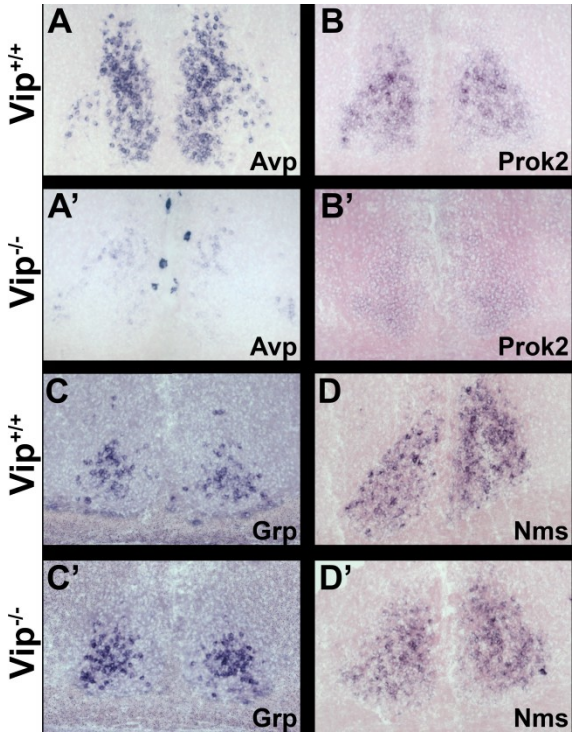

Figure 2.5: Vip effects on SCN neuropeptides. . (A-D) ISH of SCN from *Vip*$^{+/+}$ control (A-D) and *Vip*$^{-/-}$ mutant (A'-D') mice for Avp (A, A'), Prok2 (B, B'), Grp (C, C'), and Nms (D, D').

2.4 Discussion

In this study, we found that *Lhx1* deletion dramatically downregulates expression of several SCN-enriched neuropeptides crucial for circadian function (Figure 2.2). We also showed that a number of other genes with known or probable roles in neuropeptide signaling, such as neuropeptide GPCRs, Ras GTPases, adenylyl cyclase 3, and several regulators of GPCR and MAPK signaling (Table 2.1). This suggests a profound defect in the development of neuropeptidergic signaling networks in the *Six3-Cre;Lhx1*$^{lox/lox}$ SCN.

However, the expression of pan-neuronal, GABAergic interneuron and other genes broadly expressed in anterior hypothalamus is largely intact in *Six3-Cre;Lhx1*$^{lox/lox}$ SCN, as are SCN-specific genes first detectable prior to embryonic day 16.5 (E16.5) (Figures 2.3 and 2.4). This suggests that transcriptional networks regulating regional identity, neuropeptidergic and GABAergic cell fate are separate developmental programs in the SCN. This contrasts with the only other neural system where Lhx1 is known to

dictate neuropeptidergic fate; in spinal cord inhibitory interneurons, Lhx1 both drives *Npy* and *Enk* expression in conjunction with Lhx5 (Bröhl et al., 2008) and helps maintain GABAergic fate (Pillai et al., 2007). Lhx5 is not expressed in developing mammalian SCN, which may lead to Lhx1-dependent, SCN-specific expression of neuropeptides different from those in spinal interneurons (Bröhl et al., 2008).

While Lhx1 deletion also causes a comparatively moderate loss of neurons by P4 (Figures 2.3 E and 2.4 M), the region's gross anatomy remains essentially intact, with most surviving domain-specific markers retaining normal compartmentalization (Figures 2.3 A-D and 2.4 A-L). Because SCN neurogenesis is mostly complete by E16 and TUNEL revealed elevated cell death in *Lhx1*-deficient SCN between P0 and P3 (Figures 2.3 F and 2.4 N), increased neuronal apoptosis likely decreased neuron number. Apoptosis also increased between P0 and P3 in both control and mutant SCN. This is in line with the timing of peak cell death in hamster SCN, which immediately precedes innervation by the retinohypothalamic tract (Müller and Torrealba, 1998). Neuron loss does not cause SCN neuropeptide downregulation, because many neuropeptidergic populations lost in adult Lhx1-deficient SCN (*Vip*, *Avp*, *Grp*, and possibly *Prok2*) are already reduced in *Lhx1*-deficient SCN at P0, prior to neuron loss (Figures 2.3 G and 2.4 O-R). Taken together, these data indicate that increased apoptosis and neuron loss are likely secondary to defects in SCN terminal differentiation in *Six3-Cre;Lhx1*$^{lox/lox}$ SCN.

Given that Lhx1 is first detectable at E11.5 when SCN neurogenesis begins, we initially hypothesized that *Six3-Cre;Lhx1*$^{lox/lox}$ mice would have an early SCN specification defect, akin to neuronal progenitor-specific deletion of *Six3* (VanDunk et al., 2011) or constitutive deletion of *Six6* or *Lhx2* (Clark et al., 2013 and Roy et al.,

2013), rather than a terminal differentiation defect. Preservation of early-onset markers in *Lhx1* mutants suggests that any role of Lhx1 in early SCN differentiation is redundant with other factors up to E16.5. One candidate is Lhx8, a close Lhx1 homolog coexpressed with *Lhx1* in developing SCN from E11.5 until E16.5, when *Lhx8* is downregulated (Shimogori et al., 2010). Future analysis of *Lhx1*/*Lhx8* double mutants should resolve whether the latter is partially compensating for Lhx1 deletion.

More broadly, Lhx1's central role in terminal differentiation of multiple neuropeptidergic cell types in SCN presents an opportunity to dissect the transcriptional network guiding SCN cell fate determination. And indeed, this process has already begun. As I have written previously in Bedont and Blackshaw, 2015: One probable downstream component is downregulated in $Ror\alpha^{Cre/Cre};Lhx1^{lox/lox}$ SCN: the transcription factor *Creb3l1* (Hatori et al., 2014). Creb3l1 is a potent, direct regulator of *Avp* expression, whose circadian expression tracks *Avp* in adult SCN (Greenwood et al., 2014). Conversely, unlike Vip, both *Avp* and *Creb3l1* lack predicted Lhx1 binding sites in their proximal promoters (Bedont et al., 2014). Thus, Lhx1 likely indirectly controls expression of *Creb3l1* and in turn *Avp*. Our data showing a very similar level of *Avp* loss in *Six3-Cre;*$Lhx1^{lox/lox}$ and $Vip^{-/-}$ SCN (Figures 2.2 D and 2.5 A) now fills in one more link in the chain: Lhx1 controls expression of *Creb3l1* via the former's direct influence on *Vip* expression. However, one natural question this brings up for future work is whether Vip's influence on *Creb3l1* and *Avp* expression is simply a circadian effect on expression level, due to its well-known synchronizing effect on the molecular clockworks of the SCN (Aton et al, 2005; Maywood et al, 2011), or a true effect on Avp cell fate, as we previously envisioned.

Similar uncertainty lingers around another factor subsequently shown to be directly involved in control of SCN neuropeptide expression: Zfhx3 (Parsons et al, 2015). Although the ENU-produced *short-circuit* point mutation studied by the authors appears to only drive neuropeptide expression on a circadian time-scale (Parsons et la, 2015), this does not rule out a developmental role for the wild-type allele. This is particularly true given that Zfhx3 is present fairly early in SCN development and controls expression of both *Lhx1* and *Vax1*, Lhx2-controlled early markers of the SCN developmental lineage (Shimogori et al, 2010; Roy et al, 2013; Parsons et al, 2015). It is thus tempting to speculate that Zfhx3 may act upstream of Lhx1 in SCN development, a promising topic for future investigations.

2.5 Contributions

RNA preparation for RNA sequencing was carried out by Joseph Bedont. Library preparation and RNA sequencing were conducted by the staff of the Johns Hopkins Deep Sequencing and Microarray Core Facility. Analysis of RNA sequencing data was carried out by Joseph Bedont and Jonathan Ling. ISH studies were conducted by Joseph Bedont and Abhijith Bathini. IHC studies were carried out by Joseph Bedont. MOPAT analysis was conducted by Dr. Jianfei Hu.

Chapter 3: Lhx1 Regulates Circadian Functions of the SCN

Large parts of this chapter are direct excerpts and/or paraphrased passages from Bedont et al, 2014.

3.1 Introduction

Given the profound disruptions of SCN neuropeptide signaling due to the terminal differentiation defect explored in Chapter 2, we hypothesized that *Six3-Cre;Lhx1*$^{lox/lox}$ mice would have profound circadian defects. Particularly given the joint loss of Vip with a number of other neuropeptides whose signaling seems to support Vip functions in culture (Brown et al, 2005; Maywood et al, 2011), we suspected that these defects would be much more severe than in *Vip*$^{-/-}$ mice (Aton et al, 2005; Colwell et al, 2003), with interesting potential for leveraging the *Six3-Cre;Lhx1*$^{lox/lox}$ model as a tool for exploring SCN neuropeptide signaling in novel ways. We set out to test these hypotheses in the physiological and behavioral experiments described in this chapter.

3.2 Materials and Methods

Per2 Luciferase Imaging and Analysis

SCN slice cultures were created as described previously (Abe et al, 2002). Briefly, brains were removed from CO2-anesthetized and decapitated mice and placed in cold Hank's Buffered Salt Solution (HBSS). Coronal sections of the brain were sliced (300 μm thickness) with a vibratome and transferred to cold HBSS. SCN was identified under a dissecting microscope and isolated from surrounding tissue as a 1.5x1.5mm square by scalpels. SCN explants were placed on Millicell membranes (catalog #PICM030-50; pore size, 0.45 μm; Millipore, Bedford, MA) with 1 ml of DMEM (catalog #13000–021; Life Technologies, Grand Island, NY) supplemented with 10 mM

HEPES, 100 U/ml penicillin, 100 µg/ml streptomycin, B-27 serum-free supplement (catalog # 17504-044; Gibco/Life Technologies, Grand Island, NY) and 0.1 mM beetle luciferin (catalog #E1601; Promega, Madison, WI). Cultures were sealed in a 35 mm Petri dish with vacuum grease. Cultures were maintained at 36°C in darkness, and their bioluminescence was continuously monitored with a photomultiplier tube (catalog #HC135-11MOD; Hamamatsu, Shizouka, Japan) for >4 d as described previously (Geusz et al., 1997).

Seventeen additional SCN explants were placed on a single Millicell membrane using the culture conditions described above. The culture was sealed in a 35 mm Petri dish with vacuum grease and maintained in darkness at 34°C in a light-tight incubator (Onyx Box, Stanford Photonics, Inc, Palo Alto, CA). Per2::luc bioluminescence was monitored with 15 second exposures every 10 minutes for 5 days with a charge-coupled device camera (Stanford Photonics, Inc, Palo Alto, CA).

Period and amplitude of Per2::luc PMT traces were determined using modified published methods (Herzog et al, 2004). Data was detrended by subtracting 24 h running average from raw data, then analyzed by Fast-Fourier Nonlinear Least Squares, fitting for phase of the first peak, dominant period between 18-32 h, and relative amplitude. CCD images were stacked into 60-minute summed frames using Fiji software (Schindelin et al, 2012). Analysis was performed for 101 2 x 2 pixel regions of interest (ROIs) distributed in a standard array over each SCN slice. We excluded slices (1 $Lhx1^{lox/lox}$ and 3 $Six3Cre;Lhx1^{lox/lox}$) if bioluminescence was <12 counts per hour between 48-72 h of recording. We measured period and mean bioluminescence for each ROI with Chronostar V2.0 (a generous gift from A. Kramer, Charite, Berlin, Germany). All ROI periods

ranged from 18 to 32 h. Mean period and bioluminescence were calculated from 101 ROIs per SCN slice.

Clock Gene ISH Time-Course

Clock gene time course mice were entrained to LD, moved to DD for 24 hr, and sacrificed in 4 hr increments on DD day 2. Aside from this, these ISH experiments were conducted as described in Chapter 2.

Wheel-Running Behavior

Mice were housed individually with a 4.5-inch running wheel and ad libitum food and water. Wheel running was monitored using Vitalview (Mini Mitter). Photoentrainment was assayed in a 12 hr:12 hr light:dark cycle (LD). Free-running circadian rhythms were assessed in constant darkness (DD) and constant light (LL). Light intensity in LD and LL was ~600 lux, provided by Philips Daylight deluxe fluorescent lamps. Clocklab (Actimetrics) was used to generate actograms and measure circadian periods. A 3 hr light pulse from ZT 14–17 was used to measure acute activity suppression (masking) by light. Wheel revolutions were quantified during the pulse and normalized to the previous day where mice were undisturbed in the dark. A 1-week 3.5 hr:3.5 hr light:dark ultradian light cycle was also used to measure masking. Wheel revolutions were quantified to determine total activity during light and dark phases. Data were analyzed by Student's t test.

Electroencephalography (EEG) Implantation and Recording

Anesthetized mice were implanted with an EEG headmount anchored by anterior 0.1" and posterior 0.12" surgical screws (Pinnacle Technology), connected to the headmount's contact points using conductive silver epoxy and protected with a skull cap

formed of Jet Denture Repair cement (Lang Dental). After recovery from surgery, implanted mice were recorded from under a 12:12 LD cycle using a 3-channel data conditioning and acquisition system (Pinnacle Technology). Data was recorded using Sirenia acquisition software (Pinnacle Technology) and analyzed as described previously (El Helou et al, 2013; Massart et al, 2014).

X-Gal Stain

Slides were processed as described previously (Hattar et al., 2002).

Cholera Toxin Labeling

Mice were anesthetized with Avertin (20 mg/ml). Eyes were injected intravitreally with 2 µl cholera toxin B subunit (CTb) conjugated to Alexa Fluor 488 (Invitrogen). Three days later, mice were deeply anesthetized with 1 ml Avertin and transcardially perfused with 4% formalin. Brains were removed, postfixed 2 hr in 4% formalin, cryoprotected in 30% sucrose, and frozen in OCT (Tissue-Tek). Next, 50 µm sections were cut and free-floated in 0.1 M phosphate buffer, blocked (0.1 M phosphate buffer, 3% Triton X-100, 0.5% BSA, 1.5% rabbit serum) for 1 hr, incubated in goat anti-CTb (List Biologicals, 1:8,000) overnight at 4°C, and visualized with rabbit anti-goat Vectastain horseradish peroxidase kit (Vector Labs) using 3,3-diaminobenzidine (Sigma). Sections were mounted, dehydrated, and coverslipped with Permount and then viewed on a Zeiss Axio Imager M1 microscope.

Optomotry

Behavior was assessed as described previously (Chen et al., 2011). Briefly, animals were adapted for 5 min to an elevated platform centered in a virtual cylinder. A

sine wave grating was presented and acuity was assessed by the staircase method; stimulus tracking was recorded from above. Each mouse was tested in triplicate.

Pupillary Light Reflex

Behavior was assessed as described previously (Chen et al., 2011). Briefly, pupil size of one eye was video recorded for 15 s after 1 hr dark adaptation and then 30 s while the opposite eye was stimulated with a 470 nm light-emitting diode. Percent constriction relative to dark-adapted baseline was calculated from images captured from the video. Measurements were restricted to midday (ZT 4–8). Responses to low (22 μW cm2) and high (5.66 mW cm2) light intensities were recorded.

Telemetry Implantation and Recordings

G2 emitters (Starr Life Sciences) were implanted into the intraperitoneal cavity of anesthetized mice. After recovery from surgery, telemetry data was recorded under 12:12 LD and DD lighting paradigms using Vitalview software (Respironics). Clocklab (Actimetrics) was used to produce actograms and assess circadian phase and period.

Lipopolysaccharide (LPS) Studies

LPS used in this study was re-suspended in 0.9% sterile saline at a concentration of 1 mg/mL, aliquoted, and stored at -80C in siliconized Ependorfs. After entrainment to 12:12 LD and at least two weeks of subsequent free-running in DD, mice were given three daily pulses of 100 uL per 5 g of body weight10 mg/mL LPS, diluted in saline and stored on ice in siliconized Ependorfs prior to injection. The first pulse was administered at ~CT8, with the second and third pulses given at the same solar time as the initial pulse on subsequent days. After at least another two weeks in DD, another single injection of LPS was given at CT8, and the mouse's behavior was tracked for at least an additional

week. When possible, the same mice were subjected to a similar vehicle control paradigm using three days of injections with saline. Separate cohorts of mice subjected to this protocol were assessed using telemetric body temperature recordings and wheel running behavior.

Per2 Luciferase Heat Pulse Experiments

This experiment was conducted largely as described previously (Buhr et al, 2010).

Neuropeptide Cannulation Studies

Prior to injection, all mice were entrained to 12:12 LD and released into constant darkness. Wheel-running behavior of the mice was monitored, and once the mutants' activity patterns had begun to fragment, estimated CT14 was calculated for each mouse and injections were carried out. Animals were allowed to free-run for 5-7 days after each injection, long enough to allow post-injection phase angle and period to be reliably calculated. Once most mutants' activity had become too fragmented for CT to reliably be calculated, the animals were re-entrained to 12:12 LD and re-released into DD. In practice, quantitative data could only be collected from behavior before and after the first injection in each round of entrainment and release into DD; rhythms were often too degraded to quantify period and, especially, phase in mutant animals after a second injection on the same round of entrainment. Over time, the mutants' behavioral phenotype worsened, and some mutants' rhythms broke down too quickly for CT to be reliably estimated. In these cases, arrhythmic mice were injected at the same solar time as the rhythmic mouse that had most closely tracked its CT in prior rounds of entrainment and release into DD.

Human prokineticin-2 isoform 2 (H-7342, Bachem, Torrance, CA) and porcine

gastrin releasing peptide (H-1635, Bachem, Torrance, CA) were used in this study. The peptide was re-suspended in 0.9% sterile saline, aliquoted, and stored at -80C. Aliquots were thawed on ice no more than 1 h before the injection(s) for which they were used and stored on ice until immediately before use. 2 uL icv injections were given under dim red light using a syringe type microinjector (EW-07844-00, Gilmont, Libertyville, IL). The mice were then left in DD for at least 5 days post-injection, and their wheel running behavior was analyzed as described in our Methods. After Prok2 injection, heteroscedastic two-tailed t-tests were used to analyze the significance of absolute phase and period changes in Excel. Since the mutants' rhythms were less robust than controls, their estimated CTs were less accurate. In cases where post-injection rhythms were robust enough to allow it, we calculated the true CT at the injection time post-hoc and computed its correlation with the injection effect by linear regression in Excel. After Grp injection, phase and period of mutant mice often became incalculable. Thus, instead of comparing period and phase shifts, animals of either genotype without calculable phase prior to injection were excluded, and the number of remaining mutant and control animals with calculable or incalculable phase post-injection were compared using a nonparametric 2x2 Fisher's exact test in GraphPad.

Generally, investigators performing circadian cannulation studies sample a range of circadian times and neuropeptide dosages during the course of the study. In our case, this was infeasible. Only ~30% of mutants had robust enough rhythms to be cannulated in the first place, and because the mice had to regularly be re-entrained and re-released into DD over the course of the study, each injection took well over a month to perform. Furthermore, the rhythms of even Lhx1-deficient mice with relatively mild behavioral

phenotypes degraded with age, making it progressively more difficult to reliably determine the mutants' CTs as they aged. Due to these constraints, we chose to inject Prok2 at CT14 using a 114 uM injected peptide concentration, based upon the injection time and dosage shown to induce masking in a previous Prok2 icv cannulation study in wild-type rats (Cheng et al, 2002). We chose to inject Grp at CT14 using a 114 uM injected peptide concentration based upon the injection time at which maximum phase shift occurs following Grp cannulation directly into hamster SCN (Piggins et al, 1995) and our calculation that this dosage would result in a CSF concentration of exogenous Grp well within the 100 nM to 10 uM concentration range of Grp shown to maximally shift the electrophysiological rhythms of rat SCN in culture (McArthur et al, 2000).

3.3 Results

3.3.1 Synchronization of Cellular Rhythms in *Six3-Cre;Lhx1*$^{lox/lox}$ SCN

Despite profoundly decreased neuropeptide expression, bioluminescence recordings from *Six3-Cre;Lhx1*$^{lox/lox}$*;Per2*$^{luc/+}$ SCN cultures revealed clock gene rhythms with similar circadian period compared to controls from two independently tested groups of mice. Mean bioluminescence was similar in the first cohort but lower in the experimental group in the second cohort (Mann-Whitney U test, $p<0.01$). *Lhx1*-deficient SCN had reduced peak-to-trough Per2 rhythm amplitude and more rapid damping in both cohorts ($p<0.05$, Student's t test; Figure 3.1 A). Higher-resolution charge-coupled device (CCD) camera data revealed that this was attributable to reduced circadian synchrony (Figure 3.1 B) and increased circadian period variability within each *Six3-Cre;Lhx1*$^{lox/lox}$ SCN relative to controls ($p<0.001$, Student's t test; Figure 3.1 C).

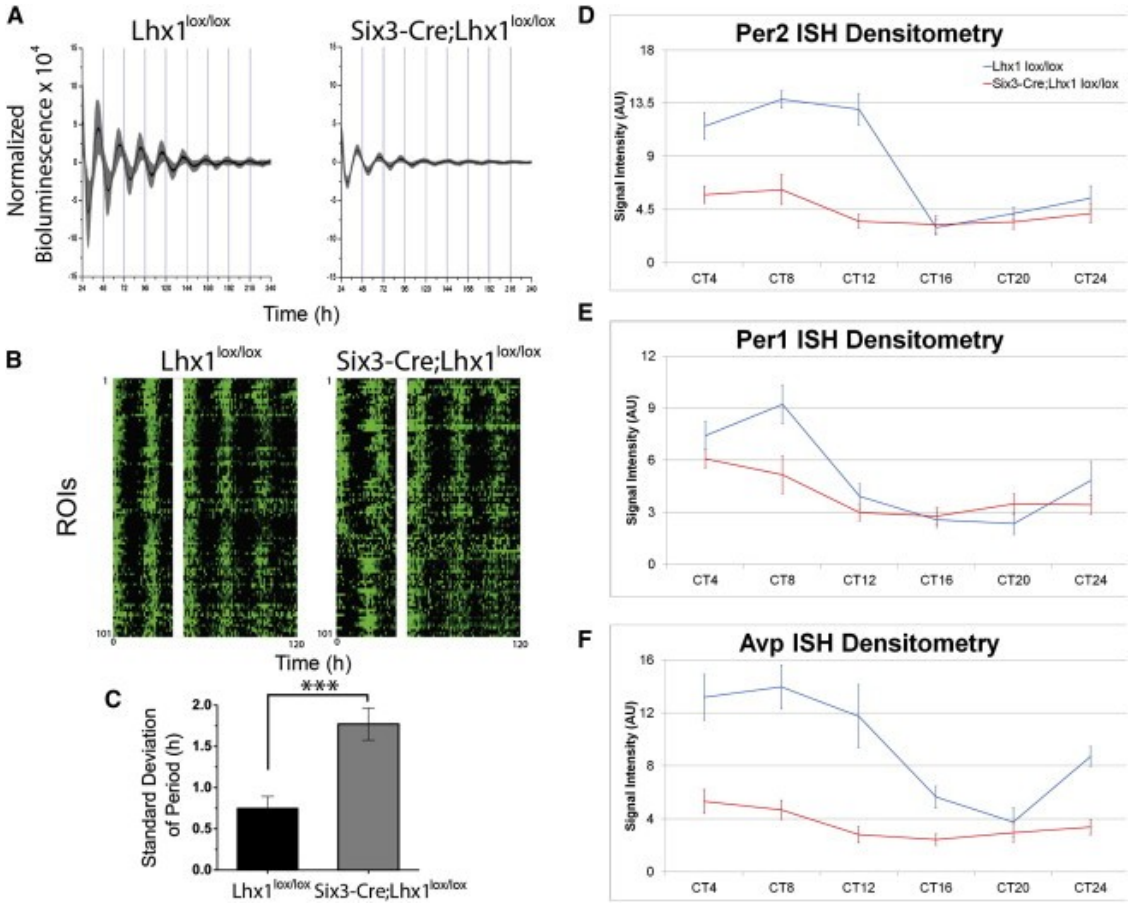

Figure 3.1: Lhx1 effects on SCN clock gene rhythms. (A) Adult *Lhx1*$^{lox/lox}$ (left) and *Six3-Cre;Lhx1*$^{lox/lox}$ (right) mouse SCN explants showed near-24 hr cycling of Per2::Luc bioluminescence over 10 days of recording, with moderately damped amplitude in the mutant explants. Traces show mean (black line) and SD (gray) of bioluminescence collected at 1 min intervals from 8 *Lhx1*$^{lox/lox}$ (left) and 9 *Six3-Cre;Lhx1*$^{lox/lox}$ (right) explants. **(B)** Raster plots demonstrate variations in synchrony of circadian rhythms across regions of interest (ROIs) from one representative control (left) and one *Six3-Cre;Lhx1*$^{lox/lox}$ SCN explant (right). White bars cover the region where data were lost while recording (40–46 hr). **(C)** Loss of *Lhx1* caused greater variance of circadian period in *Six3-Cre;Lhx1*$^{lox/lox}$ SCN explants (n = 5) compared to control littermates (n = 8). **(D–F)** Circadian variation in expression levels of SCN clock genes Per2 (D), Per2 (E), Bmal1 (C), and Avp (F). ISH labeling intensity was present in adult *Lhx1*$^{lox/lox}$ control (D–F) and *Six3-Cre;Lhx1*$^{lox/lox}$ mutant (D′–F′) mice, with genotype and interaction effects for some genes (n = 3, ANOVA).

We confirmed a similar pattern in vivo via a 24 hr ISH time course of the core clock genes *Per1* and *Per2* and the clock-controlled gene *Avp*. There were main effects of

circadian time for all three genes tested in *Six3-Cre;Lhx1*$^{lox/lox}$ SCN and controls in constant darkness (DD) (*Per1* $p<0.001$; *Per2* $p<0.0001$; *Avp* $p<0.0001$) (Figure 3.1 D-F). A main effect of genotype and an interaction were observed for *Per2* ($p<0.0001$, $p<0.01$) and *Avp* (both $p<0.0001$), but not *Per1* ($p=0.09$, $p=0.27$) (Figures 3.1 D-F). *Vip* mRNA was also examined but was virtually absent at all circadian time points (data not shown). Thus, both core clock and clock-controlled gene expression is still temporally regulated over circadian time, albeit with reduced amplitude for some genes, in the SCNs of intact *Six3-Cre;Lhx1*$^{lox/lox}$ mice.

3.3.2 Wheel Running Rhythms in *Six3-Cre;Lhx1*$^{lox/lox}$ Mice

Because lower-amplitude oscillations more readily phase shift to out-of-phase light exposure (Pulivarthy et al., 2007), we reasoned that *Six3-Cre;Lhx1*$^{lox/lox}$ animals would more readily entrain and reset to light cues than controls. Instead, activity of *Six3-Cre;Lhx1*$^{lox/lox}$ mice entrained less robustly than controls under a 12:12 light:dark cycle (LD) (Figure 3.2 A), with a small advanced phase angle of nocturnal wheel running into the light phase and a reduced percentage of overall activity confined to the dark phase (Figure 3.2 B-C). In many ways, these LD phenotypes seem similar to those seen in *Vip*$^{-/-}$ mice, leading us to initially hypothesize that Vip loss alone underpinned the behavioral deficits of *Six3-Cre;Lhx1*$^{lox/lox}$ mutants.

However, this proved incomplete when we examined the animals in DD. Despite moderate damping and desynchrony phenotypes in *Lhx1*-deficient SCN similar to or milder than previous descriptions of *Vip*$^{-/-}$ and *Vipr2*$^{-/-}$ SCN rhythms (Aton et al., 2005, Brown et al., 2007 and Maywood et al., 2011), free-running activity rhythms of Lhx1-deficient mice were profoundly disorganized (Figure 3.2 D). A total of 50% of *Six3-*

Cre;Lhx1$^{lox/lox}$ mice lacked measurable rhythms within 3 days of entry into DD, while the remainder showed two or even three distinct split rhythms, sometimes of dramatically different periods (Figure 3.2 F). In contrast, 13% of *Vip*$^{-/-}$ mice on a similar mixed background became arrhythmic within 3 days of entry into DD; this increased only to 26% of *Vip*$^{-/-}$ mice over the course of several weeks in DD (Colwell et al., 2003). A subsequent study of *Vip*$^{-/-}$ mice backcrossed to C57BL/6 found that 64% of these animals had badly disrupted rhythms, but most were multirhythmic, not arrhythmic (Aton et al., 2005).

When a behavioral rhythm is measurable, *Six3-Cre;Lhx1*$^{lox/lox}$ free-running rhythms often lacked a clearly dominant rhythm and were not of significantly different average period than controls, although individual variability in period length was markedly greater (Figure 3.2 E). This is in contrast to *Vip*$^{-/-}$ mice, which regardless of genetic background consistently have a clear dominant rhythm with a significantly shorter period than wild-type mice (Aton et al., 2005 and Colwell et al., 2003)."

"Advanced phase angle and increased activity during the LD light phase also suggested *Six3-Cre;Lhx1*$^{lox/lox}$ mice have defects in light-dependent activity suppression. Although such a decrease was supported by the observation that overall activity in constant light (LL) and DD was similar, we noticed a substantial decrease in activity in mutants under DD relative to controls (Figure 3.2 G), precluding a conclusion about masking from these data alone. To more rigorously measure masking, we first examined acute activity suppression of wheel-running activity by a 3 hr light pulse from zeitgeber time (ZT) 14–17 and found no significant difference in masking in *Lhx1*$^{lox/lox}$ and *Six3-Cre;Lhx1*$^{lox/lox}$ mice (Figure 3.4 G). We then examined masking under an ultradian light

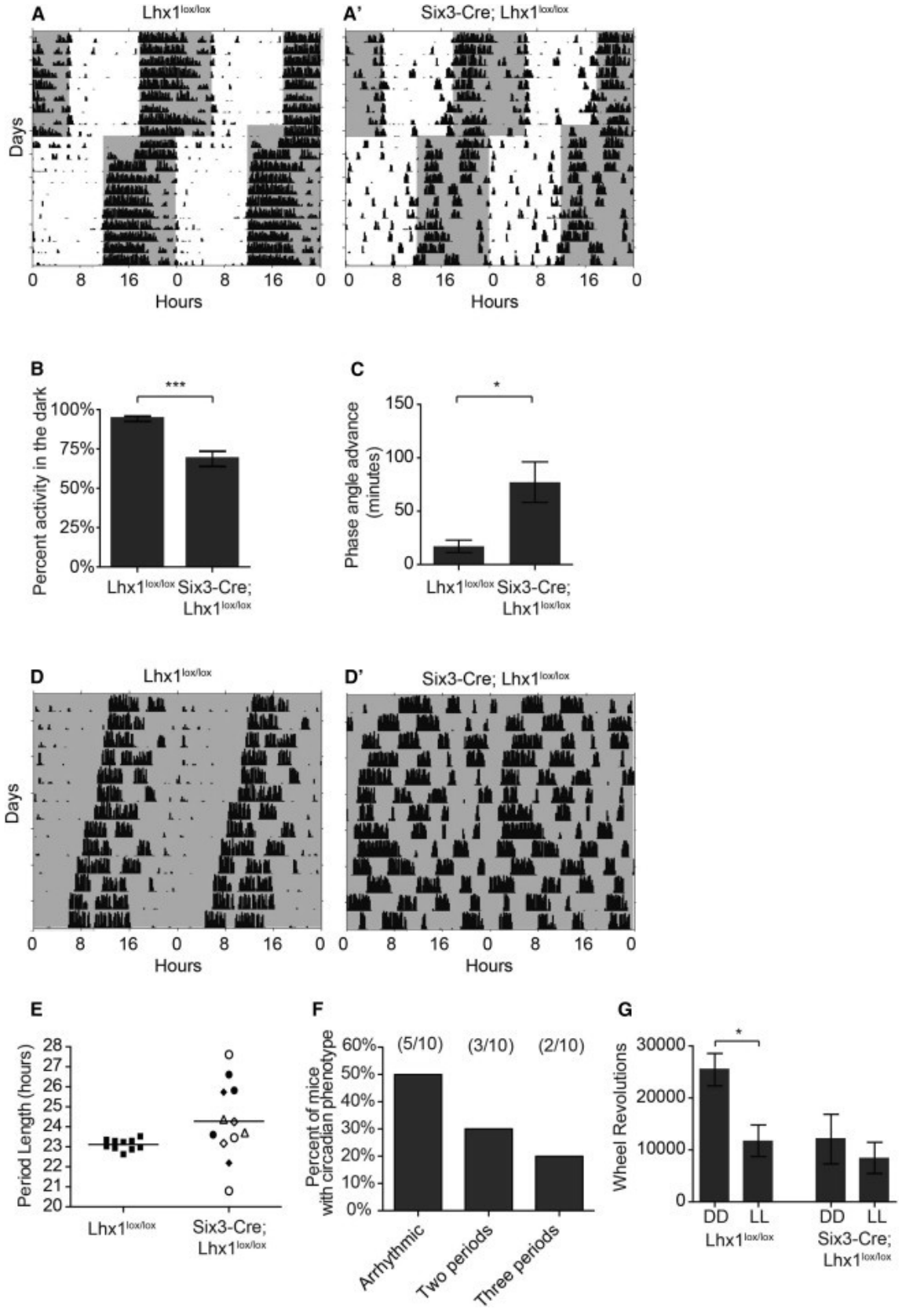
A
Lhx1lox/lox
A'
Six3-Cre; Lhx1lox/lox
Days
0 8 16 0 8 16 0
Hours
B
***
Percent activity in the dark
100%
75%
50%
25%
0%
Lhx1lox/lox
Six3-Cre; Lhx1lox/lox
C
*
Phase angle advance (minutes)
150
100
50
0
D
D'
E
Period Length (hours)
28 27 26 25 24 23 22 21 20
F
Percent of mice with circadian phenotype
60% 50% 40% 30% 20% 10% 0%
(5/10) (3/10) (2/10)
Arrhythmic
Two periods
Three periods
G
Wheel Revolutions
30000 20000 10000 0
DD LL DD LL

Figure 3.2: Loss of Lhx1 in the SCN influences photoentrainment and leads to loss of free-running circadian wheel-running rhythms. (A) Representative actograms of wheel-running activity of *Lhx1*$^{lox/lox}$ (A) and *Six3-Cre;Lhx1*$^{lox/lox}$ (A′) housed in a 12 hr:12 hr light:dark cycle and subject to a 6 hr advance in the light/dark cycle. Gray shading represents lights off. **(B)** *Six3-Cre;Lhx1*$^{lox/lox}$ mice show a decreased percentage of activity confined to the dark portion of the light/dark cycle (n=10,13; p=0.0002). **(C)** *Six3-Cre;Lhx1*$^{lox/lox}$ mice show an advanced phase angle in 12:12 LD (n=10,11; p=0.02). Data represent mean ± SEM. $^{***}p<0.001$, $^{*}p<0.05$. **(D)** Representative actograms of wheel-running activity of *Lhx1*$^{lox/lox}$ (D) and *Six3-Cre; Lhx1*$^{lox/lox}$ (D′) mice housed in constant darkness. *Six3-Cre; Lhx1*$^{lox/lox}$ mice showed either arrhythmicitiy or split rhythms under DD. **(E)** Quantification of free-running circadian period lengths in DD. Period lengths for *Six3-Cre;Lhx1*$^{lox/lox}$ are those found in mice with split rhythms. The multiple period lengths measured within a single animal are indicated by the same symbol in the mutant graph. **(F)** Distribution of circadian phenotypes observed in *Six3-Cre;Lhx1*$^{lox/lox}$ mice. **(G)** *Lhx1*$^{lox/lox}$ activity is decreased in constant light as compared to constant darkness. This difference was not observed in *Six3-Cre;Lhx1*$^{lox/lox}$ mice (n = 9–11 per group; two-way ANOVA $p_{light}=0.02$, $p_{genotype}=0.02$, Bonferroni posttest Lhx1$^{lox/lox}$ DD versus LL, $p<0.05$). Data represent mean ± SEM. $^{*}p < 0.05$.

cycle (3.5 hr light: 3.5 hr dark). Mice do not entrain to this cycle; instead, light pulses suppress wheel-running activity, permitting separation of light-masking effects from photoentrainment. The percentage of activity during the dark portion of the ultradian cycle in *Lhx1*$^{lox/lox}$ and *Six3-Cre;Lhx1*$^{lox/lox}$ mice was similar (Figure 3.4 H). Interestingly, masking does not require the SCN (Redlin and Mrosovsky, 1999), indicating that specifically SCN-mediated circadian behaviors are impaired in this mouse line. This again contrasts with *Vip*$^{-/-}$ mice, which show substantially elevated activity in response to a dark pulse (Colwell et al., 2003).

Taken together, these data show that *Six3-Cre;Lhx1*$^{lox/lox}$ mice have disrupted circadian behavior including abnormal photoentrainment and disrupted free running rhythms, with the latter seeming substantially more severe than in *Vip*$^{-/-}$ mice. However, light-dependent masking of locomotor activity is normal in our mice.

3.3.3 Sleep Rhythms in *Six3-Cre;Lhx1*$^{lox/lox}$ Mice

Circadian and light-regulated differences between the phenotypes of *Six3-Cre;Lhx1*$^{lox/lox}$ and *Vip*$^{-/-}$ mice are only accentuated when considering vigilance state characteristics of these mice as measured by EEG. Mammals show three distinct vigilance states detectable by this methodology: waking, NREMS (deep sleep), and REMS (rapid eye movement or dreaming sleep). All three states more-or-less completely lack normal circadian and light-regulated differences in their 24 hour distribution in *Six3-Cre;Lhx1*$^{lox/lox}$ mice in 12:12 LD. Thus, compared to littermate *Lhx1*$^{lox/lox}$ controls, in *Six3-Cre;Lhx1*$^{lox/lox}$ mutants waking trends higher during the day ($p<0.09$) and is lower at night ($p<0.05$), NREMS trends lower during the day ($p<0.09$) and is higher at night ($p<0.01$), and REMS is lower during the day ($p<0.05$) and higher at night ($p<0.05$). However, despite this profound disruption in the timing of sleep and wake, *Six3-Cre;Lhx1*$^{lox/lox}$ mice show no overall change in the amount of time spent in any given vigilance state over the full 24-hour day (Figure 3.3 A). In contrast, published work shows that *Vip*$^{-/-}$ mice have damped but still detectable sleep/wake rhythms, with a selective decrement in the amount of REMS they experience (Figure 3.3 B; Hu et al, 2011).

This flattening of the daily distribution of sleep in the absence of changes in overall sleep amount was also observed in *Six3-Cre;Lhx1*$^{lox/lox}$ mice for other sleep/wake parameters as well. For example, the mean duration of wakefulness bouts was not higher during the active (dark) period than during the rest (light) period as observed in control animals. This is reflected in a tendency toward higher mean duration of wakefulness bouts during the day in mutant than in control mice ($p<0.09$) and a significantly lower duration in mutant than control during the night ($p<0.05$), with no changes even in the

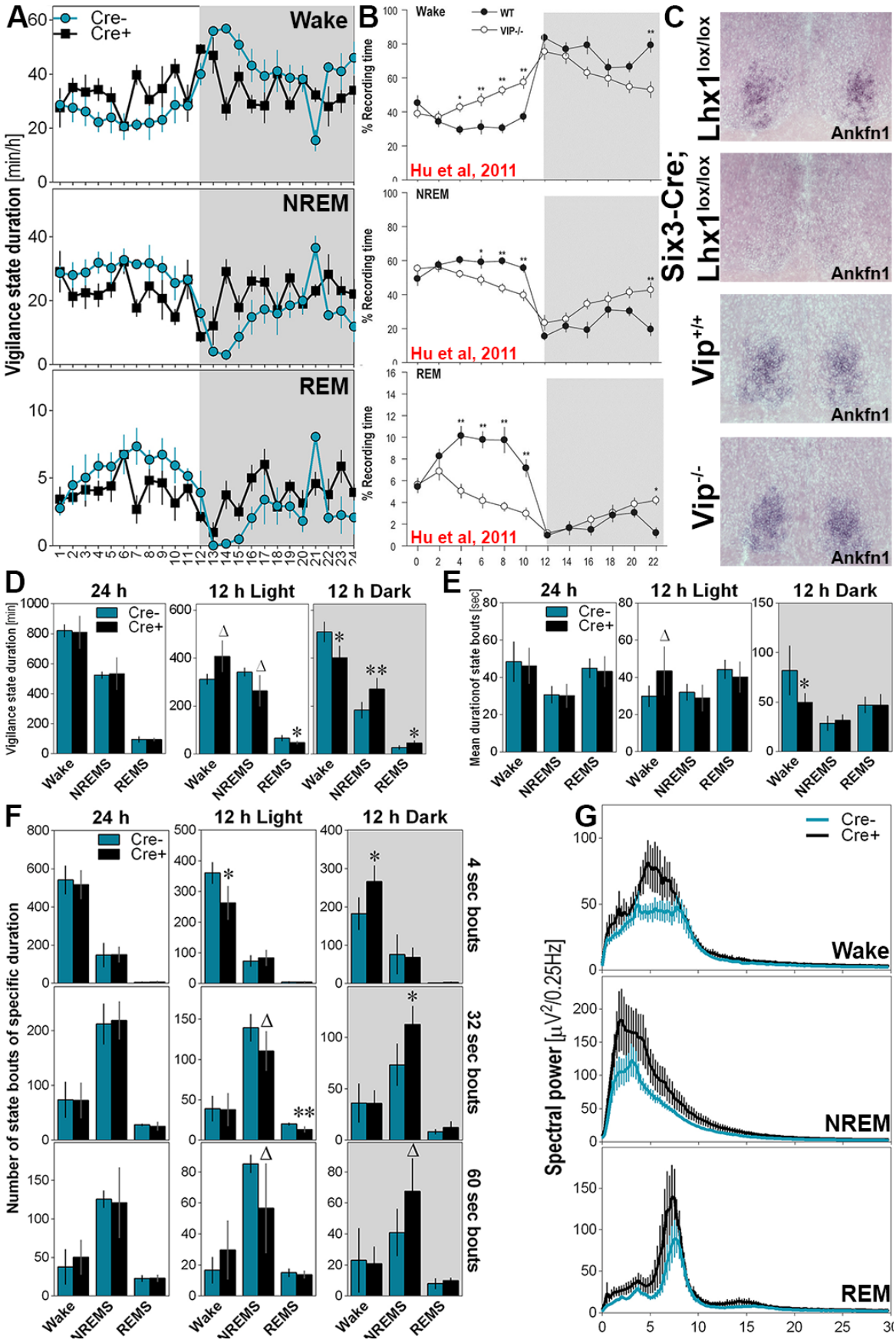
A
Cre-
Cre+
Wake
NREM
REM
Vigilance state duration [min/h]
B
Wake
WT
VIP-/-
% Recording time
Hu et al, 2011
NREM
REM
C
Lhx1lox/lox
Six3-Cre; Lhx1lox/lox
Vip+/+
Vip-/-
Ankfn1
D
24 h
12 h Light
12 h Dark
Vigilance state duration [min]
Wake
NREMS
REMS
E
Mean durationof state bouts [sec]
F
Number of state bouts of specific duration
4 sec bouts
32 sec bouts
60 sec bouts
G
Spectral power [μV²/0.25Hz]

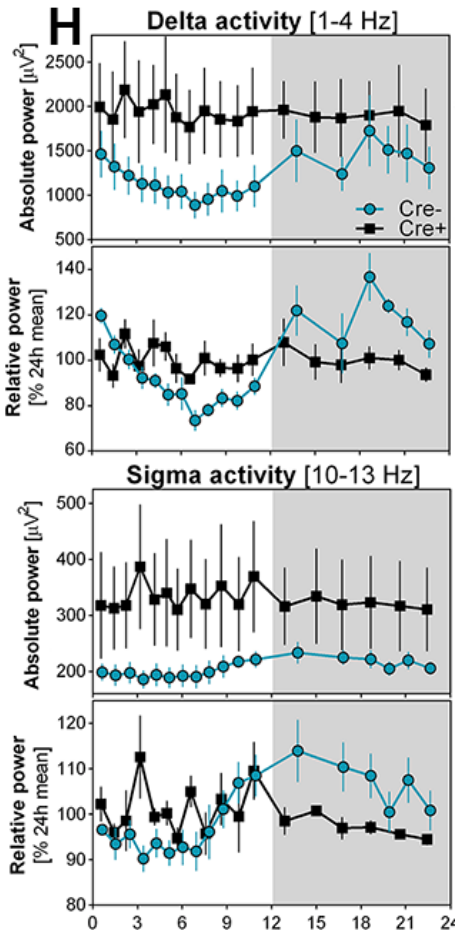

Figure 3.3 Loss of Lhx1 in the SCN abolishes both photoentrainment and free-running of vigilance state rhythms. **(A)** EEG recordings show near-complete arrhythmicity of wake, NREM, and REM sleep in 12h:12h LD (mean +/- SEM). **(B)** EEG recordings performed on *Vip*$^{-/-}$ mice by Hu et al, showing a much subtler defect in circadian control. **(C)** SCN Ankfn1 expression is disrupted by Lhx1 but not Vip deletion, providing a possible mechanism. (D) Vigilance state duration is temporally dysorganized, but otherwise unaffected, in *Six3-Cre;Lhx1*$^{lox/lox}$ mutants (mean +/- SD). **(E)** Bout duration of vigilance states is normal in *Six3-Cre;Lhx1*$^{lox/lox}$ mutants, excepting modest temporal dysregulation of waking state duration (mean +/- SD). **(F)** Short wake bouts and longer NREM bouts are temporally dysregulated in *Six3-Cre;Lhx1*$^{lox/lox}$ mutants, but the overall number of bouts of each length are unchanged (mean +/- SD). **(G)** EEG spectra during wake, REM, and NREM (mean +/- SEM). **(H)** Both delta and sigma activity are essentially arrhythmic in *Six3-Cre;Lhx1*$^{lox/lox}$ mutants. Absolute power also appears to be elevated (mean +/- SEM). (delta $p<0.09$; * $p<0.05$; ** $p<0.01$)

temporal distribution of REMS and NREMS across the active and rest phases (Figure 3.3 E). The overall amounts of all three states, however, were the same, reflecting essentially wild-type consolidation of sleep and wake states in *Six3-Cre;Lhx1*$^{lox/lox}$ mice despite their profound temporal disorganization.

Similarly, the number of bouts of given length showed some daily variations in *Six3-Cre;Lhx1*$^{lox/lox}$ mice (Figure 3.3 F). They had fewer very short 4 sec bouts of waking during the day and more at night compared to controls ($p<0.05$), and tended to have fewer relatively long 32 and 60 second bouts of NREMS during the day and more at

night ($p<0.09$). However, the number of bouts of all lengths were the same for all vigilance states when considered across the solar cycle.

The profound temporal disorganization of these mutants held true even when considering the spectral power of *Six3-Cre;Lhx1*$^{lox/lox}$ EEG recordings. Relative delta and sigma activity were essentially flat across the solar cycle in *Six3-Cre;Lhx1*$^{lox/lox}$ mice compared to controls (Figure 3.3 G-H). That said, the absolute EEG signal for *Six3-Cre;Lhx1*$^{lox/lox}$ mice was higher across most spectra compared to controls, but this did not reflect a change in the overall amount of any specific frequency (Figure 3.3 G-H).

3.3.4 Intact ipRGC Innervation of SCN After *Lhx1* Deletion

We utilized the *Opn4tau-LacZ* mouse to selectively label ipRGCs by X-gal staining (Güler et al., 2008 and Hattar et al., 2002). *Six3-Cre;Lhx1*$^{lox/lox}$;*Opn4*$^{taulacZ/+}$ mutants and *Lhx1*$^{lox/lox}$;*Opn4*$^{taulacZ/+}$ controls had similar gross innervation of SCN, olivary pretectal nucleus, and lateral geniculate nucleus (Figure 3.4 A-B). This was corroborated by labeling all RGCs using intravitreal cholera toxin tract tracing in *Six3-Cre;Lhx1*$^{lox/lox}$ mice and controls (Figure 3.4 C-D). We then measured pupillary light reflex and visual acuity (optokinetic response) to assess the function of ipRGCs and RGCs, respectively. We found that ipRGCs are functional in *Six3-Cre;Lhx1*$^{lox/lox}$ mice, because pupillary light reflex was comparable to controls under both dim and bright light (Figure 3.4 E). *Six3-Cre;Lhx1*$^{lox/lox}$ mice also show an optokinetic response, but we observed a small but significant reduction in visual acuity (Figure 3.4 F). This is likely due to defects in horizontal cell lamination known to occur after Lhx1 deletion in the developing retina (Poché et al., 2007), which is targeted by our Cre driver (Furuta et al., 2000). Lhx1 does not play a specific role in the development of any other retinal cell type. Taken together,

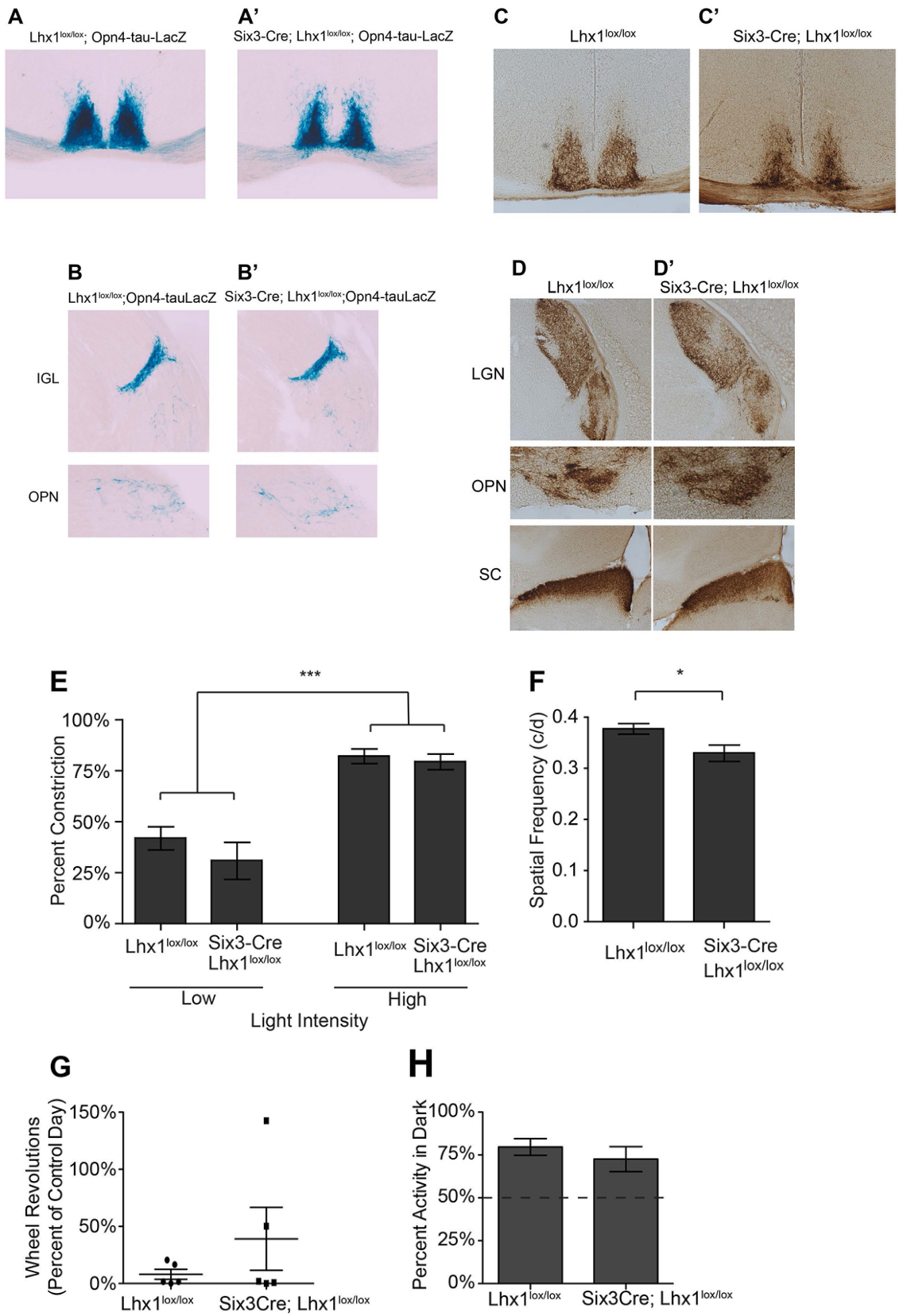
A
Lhx1lox/lox; Opn4-tau-LacZ
A'
Six3-Cre; Lhx1lox/lox; Opn4-tau-LacZ
C
Lhx1lox/lox
C'
Six3-Cre; Lhx1lox/lox
B
Lhx1lox/lox;Opn4-tauLacZ
B'
Six3-Cre; Lhx1lox/lox;Opn4-tauLacZ
IGL
OPN
D
Lhx1lox/lox
D'
Six3-Cre; Lhx1lox/lox
LGN
OPN
SC
E
***
Percent Constriction
100%
75%
50%
25%
0%
Lhx1lox/lox
Six3-Cre Lhx1lox/lox
Lhx1lox/lox
Six3-Cre Lhx1lox/lox
Low
High
Light Intensity
F
*
Spatial Frequency (c/d)
0.4
0.3
0.2
0.1
0.0
Lhx1lox/lox
Six3-Cre Lhx1lox/lox
G
Wheel Revolutions (Percent of Control Day)
150%
100%
50%
0%
Lhx1lox/lox
Six3Cre; Lhx1lox/lox
H
Percent Activity in Dark
100%
75%
50%
25%
0%
Lhx1lox/lox
Six3Cre; Lhx1lox/lox

Figure 3.4: ipRGC input and behavioral masking are intact in *Six3-Cre;Lhx1$^{lox/lox}$* Mice. (A) ipRGCs projections (shown in blue) to the SCN are intact in *Lhx1$^{lox/lox}$;Opn4$^{tau-LacZ}$* and *Six3-Cre;Lhx1$^{lox/lox}$;Opn4$^{tau-LacZ}$* mice. **(B)** ipRGC projections to IGL and OPN are intact in *Lhx1$^{lox/lox}$;Opn4$^{tau-LacZ}$* and *Six3-Cre;Lhx1$^{lox/lox}$;Opn4$^{tau-LacZ}$* mice. **(C)** Pupillary light reflex is intact in *Six3-Cre;Lhx1$^{lox/lox}$* mice and comparable to controls (n=10-11 per group, per group , $p<0.0001$). Data represent Mean ± SEM ***$p<0.0001$. **(D-E)** Cholera toxin labeling shows intact retinal projections (shown in brown). **(F)** *Six3-Cre;Lhx1$^{lox/lox}$* mice show a small defect in visual acuity in the optomotor task (n=8,10 per group, $p=0.03$). Data represent Mean ± SEM *$p<0.05$. **(G)** No difference was observed in masking in response to a 3-hour masking pulse (*Lhx1$^{lox/lox}$*: 0.08 ± 0.04, n=5; *Six3-Cre;Lhx1$^{lox/lox}$*: 0.39± 0.28, n=5) or **(H)** T7 light cycle (*Lhx1$^{lox/lox}$*: 0.76 ± 0.03, n=16; *Six3-Cre;Lhx1$^{lox/lox}$*: 0.71± 0.04, n=13). Mice in T7 confined their activity to the dark phase (One sample t-test $\mu=50\%$: $p=0.0037$, 0.0361). Horizontal line (G) and Bars (H) represent mean. Error bars represent SEM.

these results suggest that deficits in locomotor activity [and vigilance state] of *Six3-Cre;Lhx1$^{lox/lox}$* mice were not a result of abnormal retinal input to the SCN."

3.3.5 Temperature Entrainment of *Six3-Cre;Lhx1$^{lox/lox}$* Mice

(*Note: this study is ongoing, and all data described herein are provisional.*)

It has been shown in slice culture that the SCN's core clock gene expression rhythms resist changes in temperature, a cue which can readily reset and entrain peripheral tissues (Buhr et al, 2010). While inhibiting Vip and Avp alone only increase the standard deviation of SCN responses to heat, applying tetrodotoxin or cleaving apart the SCN core and shell domains allows for robust resetting and entrainment of the SCN by heat (Buhr et al, 2010). However, since an SCN entrained to heat by prolonged exposure to 12:12 temperature cycles more readily phase-shifts to this cue when accompanied by exogenous Vip (An et al, 2013), and given that the core/shell severing paradigm used by Buhr et al separates several key neuropeptidergic populations from each other, it seemed likely to us that SCN resistance to circadian manipulation by

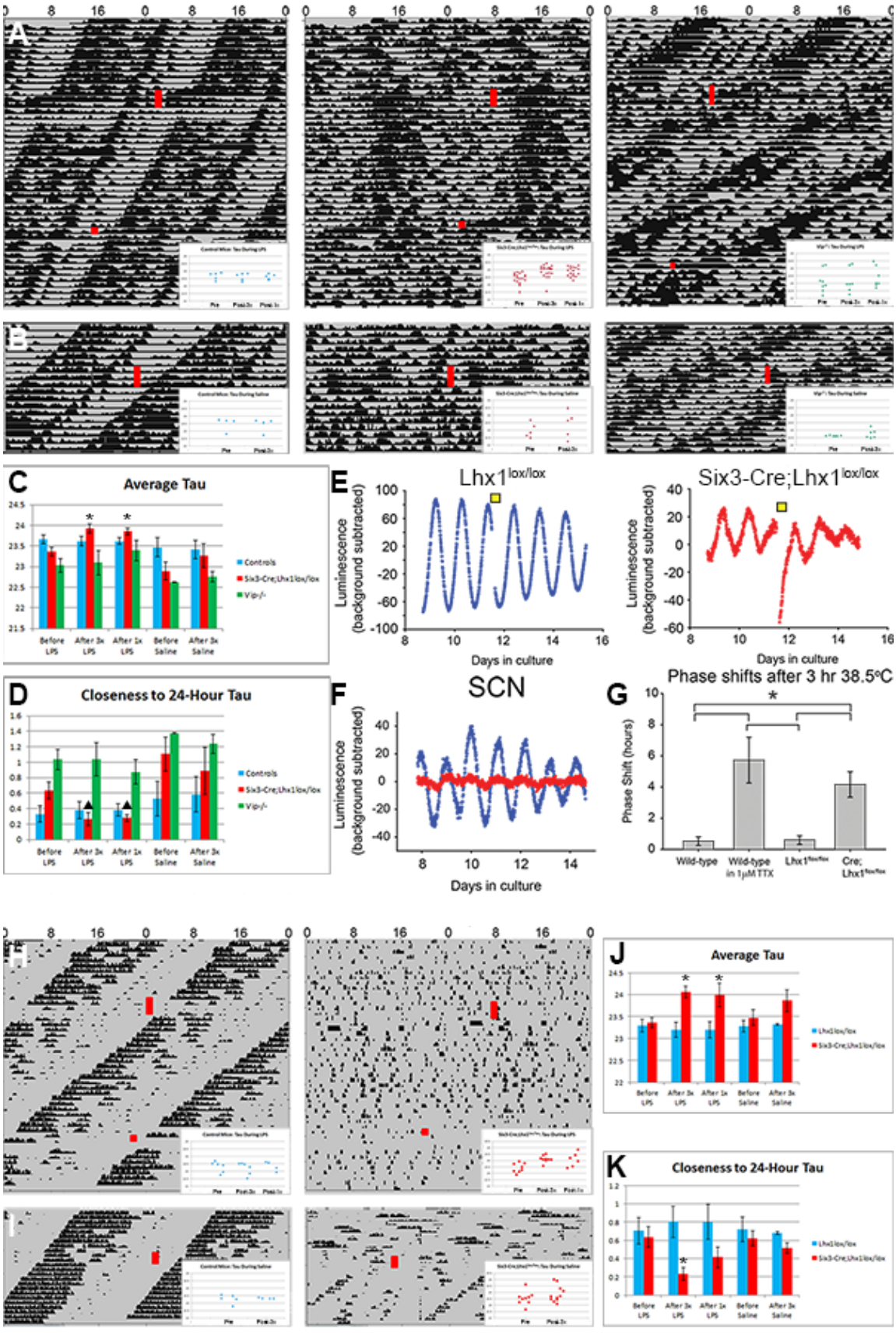
A
B
C
Average Tau
Controls
Six3-Cre;Lhx1lox/lox
Vip-/-
Before LPS
After 3x LPS
After 1x LPS
Before Saline
After 3x Saline
D
Closeness to 24-Hour Tau
E
Lhx1lox/lox
Six3-Cre;Lhx1lox/lox
Luminescence (background subtracted)
Days in culture
F
SCN
G
Phase shifts after 3 hr 38.5°C
Phase Shift (hours)
Wild-type
Wild-type in 1μM TTX
Lhx1lox/lox
Cre; Lhx1lox/lox
H
I
J
Average Tau
K
Closeness to 24-Hour Tau

Figure 3.5: Temperature entrainment of *Six3-Cre;Lhx1$^{lox/lox}$* core body temperature and wheel running rhythms using fever. **(A)** Sample core body temperature recordings from control (left), *Six3-Cre;Lhx1$^{lox/lox}$* (middle), and *Vip$^{-/-}$* (right) mice, before and after 3 days of LPS injections (long rectangle) and 1 LPS injection (short rectangle). Scatter plots in bottom right show the period of each individual rhythm. **(B)** As A, but before and after 3 days of saline injections. **(C)** Temperature tau of *Six3-Cre;Lhx1$^{lox/lox}$* increased by 3x LPS injection. **(D)** Tau of Six3-Cre;Lhx1lox/lox temperature rhythms trends toward 24 hours after 3x LPS injection. **(E/F)** Per2::Luc photomultiplier tube recordings show a marked phase shift in *Six3-Cre;Lhx1$^{lox/lox}$* after temperature pulse (yellow rectangle). **(G)** This phase shift is similar to that seen after wild-type SCN incubation in TTX. **(H/I)** Sample actograms and period scatter plots of wheel-running behavior, using the same LPS and saline protocols as in A/B. **(J)** Average temperature tau of *Six3-Cre;Lhx1$^{lox/lox}$* trends higher after 3x LPS injection. **(K)** Tau of *Six3-Cre;Lhx1$^{lox/lox}$* temperature rhythms significantly closer to 24 hours after 3x LPS; this difference is lost after 1x LPS. (all bar graphs mean +/- SEM) (delta $p<0.10$, * $p<0.05$).

temperature was rooted in the overall neuropeptide network, of which Vip is a part but far from the whole story. We tested this hypothesis by attempting to entrain *Six3-Cre;Lhx1$^{lox/lox}$*, *Vip$^{-/-}$*, and control mice using lipopolysaccharide (LPS) induced fever. To our knowledge, this experiment also represented the first explicit *in vivo* test of whether SCN rhythms' resistance to temperature disruption is necessary for the resistance of an intact mouse's circadian rhythms of behavior to the same cue.

And indeed, the temperature rhythms of *Six3-Cre;Lhx1$^{lox/lox}$* mice are readily entrainable by three consecutive days of LPS injections (Figure 3.5 A Middle). Their periods are significantly elongated ($p<0.05$), trending toward an average duration of 24 hours ($p<0.10$) (Figure 3.5 C-D). We also observed a robust consolidation of rhythms in a subset of *Six3-Cre;Lhx1$^{lox/lox}$* mice after this manipulation; our efforts to determine the factor(s) distinguishing consolidators from non-consolidators are ongoing. A single LPS pulse was insufficient to reset the change in temperature rhythm period after the triple

pulse, with period staying largely the same afterward (Figure 3.5 C-D), but was sufficient to deconsolidate temperature rhythms in animals that were consolidated by the triple pulse.

In contrast, much like SCN slices exposed to Vip antagonist (Buhr et al, 2010), *Vip*$^{-/-}$ mice showed scattershot changes in period in response to both LPS triple pulse and single pulse, but neither stimulus produced the kind of robust period setting or consolidating effects seen in *Six3-Cre;Lhx1*$^{lox/lox}$ mice (Figure 3.5 A right,C,D). And as expected, control mice experienced no lasting circadian effects from either LPS stimulus (Figure 3.5 A left,C,D). Saline vehicle control injections failed to produce a coherent period or consolidation phenotype in any of the genotypes examined (Figure 3.5 B-D).

Wheel running activity rhythms in *Six3-Cre;Lhx1*$^{lox/lox}$ mice were affected similarly by this LPS paradigm (Figure 3.5 H right). Their periods were significantly elongated after the LPS triple pulse (Figure 3.5 J; $p<0.05$), due to a significant movement of the average tau toward 24 hours (Figure 3.5 K; $p<0.05$). In this case, unlike the temperature rhythms, the LPS single pulse was sufficient to at least partially reset period; though the average period remained elongated relative to baseline (Figure 3.5 J; $p<0.05$), it was no longer significantly closer to an average of 24 hours after this resetting stimulus (Figure 3.5 K). Consolidation of *Six3-Cre;Lhx1*$^{lox/lox}$ wheel-running activity, when it occurred, appeared somewhat less robust than in the temperature recordings, but was still disrupted by the single LPS pulse (Figure 3.5 H). As in the temperature recordings, saline vehicle injections had no effect (Figure 3.5 I-K).

Finally, given the many immunological effects of LPS, we sought to determine if the SCN was really more susceptible to heat, rather than some other aspect of the LPS

response. For this experiment, we exposed *Six3-Cre;Lhx1*$^{lox/lox}$*;Per2*$^{luc/+}$ and *Lhx1*$^{lox/lox}$*;Per2*$^{luc/+}$ brain slices to a single heat pulse (the minimal temperature insult used in Buhr et al, 2010) and recorded the effect. As expected from our *in vivo* data, this stimulus robustly phase shifted SCN rhythms, in a manner statistically indistinguishable from wild-type brain slices heat shifted during exposure to tetrodotoxin (Figure 3.5 E-G).

3.3.6 Neuropeptide Cannulation in *Six3-Cre;Lhx1*$^{lox/lox}$ Mice

Given the low-amplitude but persistent molecular and cellular rhythms in *Lhx1*-deficient SCN, we hypothesized that an in vivo pulse of Grp, known to synchronize disorganized SCN cellular oscillators in culture (Brown et al., 2005 and Maywood et al., 2011), should consolidate our mutants' behavioral rhythms. To allow approximate calculation of circadian time (CT) for the injections, we selected *Six3-Cre;Lhx1*$^{lox/lox}$ mice exhibiting the mildest subset of splitting phenotypes, including one exceptional mouse that usually exhibited essentially wild-type behavior, for our cannulation studies (Figures 3.6 A-B).

We first determined that an intracerebroventricular (i.c.v.) saline injection produced no effect regardless of genotype (Figure 3.6 A). Control mice exhibited phase shifts after Grp cannulation (-0.55 hr $\pm$ 0.26, $p < 0.05$, one-tailed paired Student's t test), consistent with previous work (Piggins et al., 1995) (Figures 3.6 B). Acute inhibition of locomotion was also often observed. Surprisingly, visual inspection of actograms from *Six3-Cre;Lhx1*$^{lox/lox}$ mice after i.c.v. Grp injection showed considerable deconsolidation of activity rhythms (Figures 3.6 B′). To quantify this, we compared the number of animals of both genotypes with measurable circadian phase before, but not following, Grp administration. We found a significant deleterious effect of Grp on mutant activity

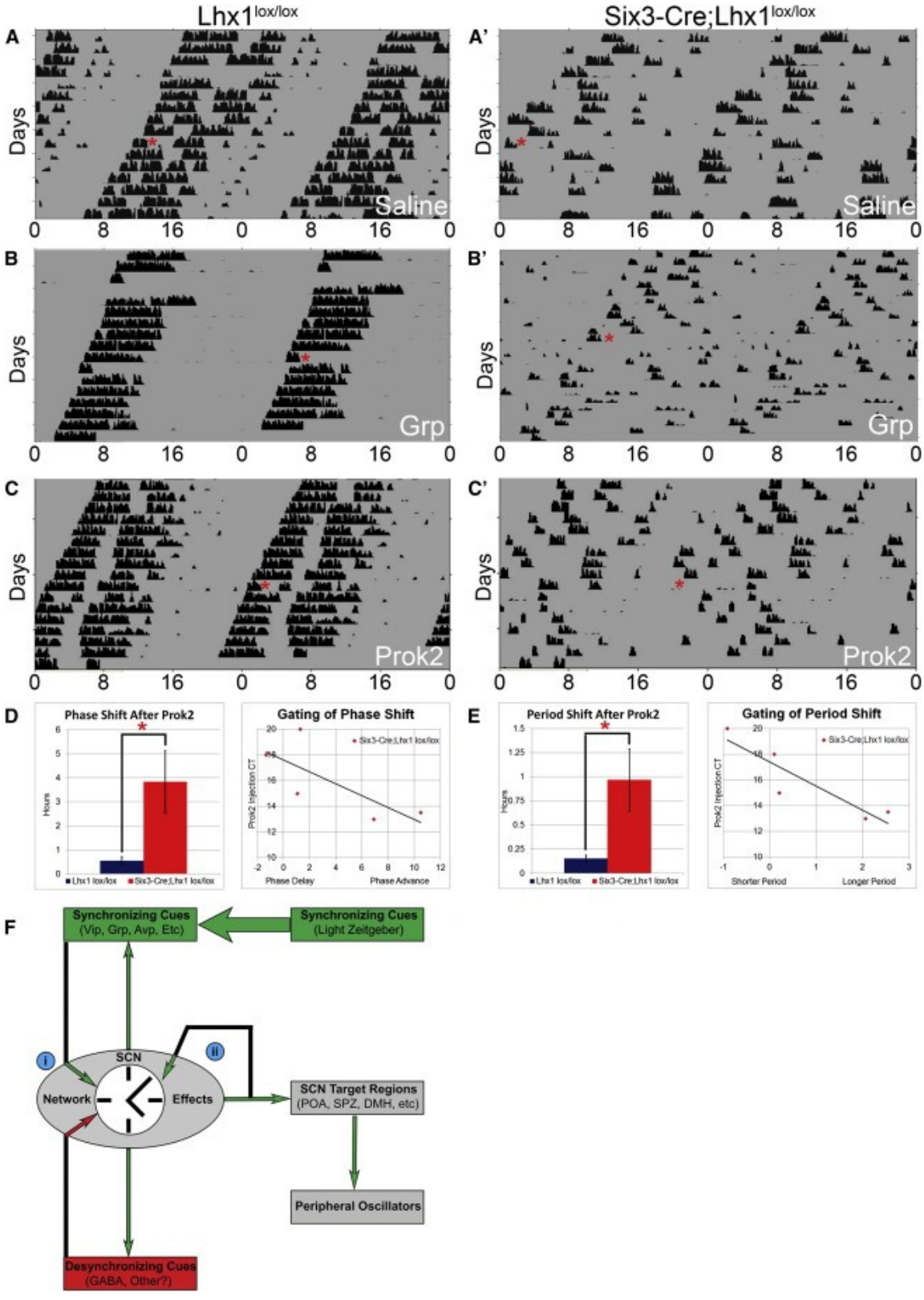
Lhx1lox/lox
Six3-Cre;Lhx1lox/lox
A
A'
B
B'
C
C'
Days
Saline
Grp
Prok2
0
8
16
D
E
F
Phase Shift After Prok2
Gating of Phase Shift
Period Shift After Prok2
Gating of Period Shift
Hours
Prok2 Injection CT
Phase Delay
Phase Advance
Shorter Period
Longer Period
Lhx1 lox/lox
Six3-Cre;Lhx1 lox/lox
Synchronizing Cues
(Vip, Grp, Avp, Etc)
Synchronizing Cues
(Light Zeitgeber)
SCN
Network
Effects
SCN Target Regions
(POA, SPZ, DMH, etc)
Peripheral Oscillators
Desynchronizing Cues
(GABA, Other?)

Figure 3.6: The *Lhx1*-deficient circadian system is hypersensitive to cannulation of the SCN output molecule Prok2. (A–C) Representative actograms of wheel-running activity of *Lhx1*$^{lox/lox}$ (A–C) and *Six3-Cre;Lhx1*$^{lox/lox}$ (A′–C′) mice before and after an i.c.v. injection (red asterisk) of saline (A), Grp (B), or Prok2 (C) in DD. **(D/E)** Mutants had higher-magnitude phase shifts (D) and period shifts (E) in response to Prok2 than controls (left) (n = 8, two-tailed heteroscedastic t tests, $^{*}p < 0.05$; bar graphs depict mean ± SEM). Both phase and period shifts in mutants were gated by injection CT (right) (n = 5, linear regression, scatterplots depict CT versus phase or period shift of individual injections). **(F)** A model of SCN neuropeptide dynamics. Synchronizing factors are shown in green, desynchronizing factors are shown in red, and factors without clear implications for synchrony are shown in black. The following insights gained from our study are highlighted: (i) synchronizing and desynchronizing effects of SCN signals like Grp can be contingent on interpretation by the broader network, and (ii) coreneuropeptides may buffer circadian period length, stabilizing it in the face of feedback signaling from SCN outputs like Prok2 that would otherwise alter it.

rhythms (postinjection phase measurable after 7/7 control injections versus 1/5 mutant injections, Fisher's exact test, p = 0.01).

Given the dramatic deconsolidating effect of Grp, we hypothesized that *Lhx1*-deficient SCN might be sensitive to pulses of SCN output neuropeptides that do not normally produce phase changes in wild-type animals. We tested this by i.c.v. injection of the SCN output neuropeptide Prok2. We found that i.c.v. Prok2 cannulation acutely inhibited locomotion without affecting either phase or period in control mice, as previously observed in rat (Figures 3.6 C; Cheng et al., 2002). Remarkably, Prok2 significantly altered not just phase but also period in *Six3-Cre;Lhx1*$^{lox/lox}$ mice ($p < 0.05$; Figures 3.6 C–E). Period shift after a single injection often lasted for many cycles. When rhythms were robust enough to calculate a more accurate post hoc circadian time of the injection (5/8 injections), there was clear circadian gating of both period shift (r2 = 0.82)

and phase shift (r2 = 0.56), with the largest shifts occurring closest to the target injection time of CT14 (Figure 3.6 D-E).

3.4 Discussion

Despite loss of expression of multiple neuropeptides involved in synchronization of SCN oscillators in *Six3-Cre;Lhx1*$^{lox/lox}$ mice, rhythms of Per2::luciferase expression in SCN slice cultures showed normal average period and only moderately damped amplitude (Figure 3.1 A). CCD imaging showed this was due to reduced cellular synchrony and increased period variability in *Lhx1*-deficient SCN (Figure 3.1 B-C). Furthermore, our ISH time course showed that clock and clock-controlled gene expression is still temporally regulated in vivo after *Lhx1* deletion (Figures 3.1 D–F). These deficits are similar to what has been observed shortly after culturing *Vipr2*$^{-/-}$ SCN slices (Brown et al., 2007).

The severe circadian deficits in *Six3-Cre;Lhx1*$^{lox/lox}$ DD activity rhythms were unexpected given the moderate effects on SCN oscillators in these animals (Figures 3.1 and 3.2). Although some mutants had milder splitting phenotypes (Figures 3.2 F), most had multiple rhythms with distinct periods or had no measurable rhythms at all (Figures 3.2 D-F). Typically, behavioral rhythms are more, not less, well organized than those of cellular clocks (Aton et al., 2005, Colwell et al., 2003 and Harmar et al., 2002), making our observations unusual. Severe behavioral disorganization, normal average circadian period, a lack of altered activity rhythm masking by darkness, and the disconnect between robustness of cellular and behavioral rhythms all suggest that the phenotype of *Lhx1* deletion in SCN is not simply a product of Vip loss (Aton et al., 2005 and Colwell et al., 2003).

The most likely explanation rationalizing our SCN clock and behavioral data is that loss of expression of SCN neuropeptides following *Lhx1* deletion leads the SCN to become not only internally disorganized but also uncoupled from downstream oscillators in the absence of external light cues. This suggests that Lhx1-regulated neuropeptide(s) and/or other signals could constitute the unidentified paracrine signals proposed to be sufficient for synchronization of peripheral oscillators by SCN (Silver et al., 1996). Prok2 is one likely component, because *Prok2*$^{-/-}$ SCN also seems to have a reduced ability to drive circadian rhythms (Li et al., 2006); however, the low percentages of *Prok2*$^{-/-}$ mice with severely disrupted rhythms (13% in mixed background and 20% after backcrossing to C57BL/6) suggest that it alone cannot account for the entirety of the *Six3-Cre;Lhx1*$^{lox/lox}$ phenotype. On the other hand, phase-advanced photoentrainment in *Six3-Cre;Lhx1*$^{lox/lox}$ mice, with an activity onset before dark, suggests that the *Lhx1*-deficient SCN does engage downstream oscillators when driven by light. Light entrainment may coordinate remaining SCN outputs, such as GABA (Moore and Speh, 1993), to preserve activity rhythms under light-dark conditions.

However, even under LD, the distribution of vigilance states across solar time as measured by EEG is essentially flat in *Six3-Cre;Lhx1*$^{lox/lox}$ mice, in contrast to the modest defects of photoentrainment seen in wheel-running activity rhythms (Figures 3.2 and 3.3). This remains true regardless of whether the overall amount of time spent in, bout length of, or number of bouts of the three major vigilance states (wake, NREMS, and REMS), or spectral power are considered (Figure 3.3). The flattening we observe appears more profound than that previously reported for *Vip*$^{-/-}$ mice (Hu et al, 2011), instead appearing much more similar to the arrhythmic phenotype with robust ultradian rhythms present in

many individual animals that is seen after complete SCN lesion (data not shown; Eastman et al, 1984). Excitingly, the phenocopy of SCN lesioned EEG patterns in our study, which eliminates the confound of extensive retinohypothalamic tract damage in the earlier work by Eastman et al (1984) (Figure 3.4), allows us to extend the existing hypothesis of separate circadian and light-driven, clock-independent SCN pathways from the regulation of peripheral rhythms (Husse et al, 2014) to include temporal regulation of vigilance state (and perhaps body temperature rhythms, which we have not focused on in this thesis but show an intermediate amount of disorganization in LD compared to sleep and wheel-running) as well. In contrast, our work on wheel-running rhythms in *Six3-Cre;Lhx1*$^{lox/lox}$ mice do not support the extension of Husse et al's two pathway model to activity rhythms at this time, though because of the confound of potential entraining effects of the wheel, we cannot rule it out.

The extremely strong relative phenotype observed in our mutants may be explained at least in part by the loss of *Ankfn1* in *Six3-Cre;Lhx1*$^{lox/lox}$ but not *Vip*$^{-/-}$ mice (Figure 3.3 C). Although not yet decisive, this tempting possibility supports a conserved role of *Ankfn1* in mammals similar to *wide awake*'s coupling of the circadian clock to sleep in Drosophila (Liu et al, 2014), and perhaps also to direct light control of the process as well. Future studies with *Ankfn1* loss-of-function mice will be required to address this mechanistic point definitively.

Conversely, *Six3-Cre;Lhx1*$^{lox/lox}$ mutants do not show a decrease in the overall amount of REM sleep seen in *Vip*$^{-/-}$ mice, nor do *Six3-Cre;Lhx1*$^{lox/lox}$ mutants show the light:dark differences in average NREM and REM sleep bout duration seen in *Vip*$^{-/-}$ mice (Hu et al, 2011). These milder phenotypes may simply indicate that these changes in

sleep parameters in *Vip*$^{-/-}$ mice are due to a role of Vip outside the SCN. However, a more interesting possibility is that it may indicate a multi-actor "tug of war" in the SCN in regards to sleep, with Vip and other signal(s) selectively lost in *Six3-Cre;Lhx1*$^{lox/lox}$ SCN pulling in opposite directions to modulate the amount of REM sleep and/or duration of NREM and REM bouts. These possibilities could readily be distinguished by future studies selectively deleting *Vip* in the murine SCN.

Finally, we have attempted to move beyond simply characterizing the behavioral phenotypes of the developmental defects we observe in *Six3-Cre;Lhx1*$^{lox/lox}$ mice. The loss of so many neuropeptide signals cannot easily be accomplished by targeting the genes individually, and we believe that this system affords us unique opportunities to interrogate the physiology of the SCN.

The first such topic was addressing the role of the SCN neuropeptide network in controlling the resistance of not just the local molecular clock, but the intact organism, to temperature entrainment and resetting. Given data suggesting that blockade of single neuropeptide signals such as Vip and Avp cannot render the SCN susceptible to this in slice (Buhr et al, 2010), but that addition of Vip can speed phase shifts in SCN already forced over the course of many days to entrain to temperature (An et al, 2013), it seemed probable to us that an extensive neuropeptide network including Vip acts together to convey this resistance *in slice*. However, to date, no one had shown that this SCN resistance was indeed necessary for an intact mouse's ability to resist behavioral entrainment by temperature stimuli. *Six3-Cre;Lhx1*$^{lox/lox}$ mice presented a natural model to attempt to translate these results these results to the intact mouse.

Our findings that LPS can entrain *Six3-Cre;Lhx1*$^{lox/lox}$ but not *Vip*$^{-/-}$ mice (Figure 3.5 A-D, H-K) validate the relevance of these slice studies for intact organisms. Furthermore, the statistically similar susceptibility of *Lhx1*-deficient and tetrodotoxin-treated SCNs to temperature resetting suggest that Lhx1-regulated factors (likely, neuropeptides) mediate the bulk of this resistance (Figure 3.5 E-G). Together, these findings have interesting biological and public health implications.

To begin, the relatively late and staggered onset of neuropeptide expression throughout late embryonic and early post-natal life (reviewed in Bedont and Blackshaw, 2015) may leave pups' SCN resistance to temperature cues in utero weak enough for maternal core body temperature rhythms to play a role in entrainment of their rhythms. Conversely, decoupling of the SCN from downstream oscillators and down-regulation of neuropeptide expression in the presence of a relatively functional SCN core clock is known to occur in normal aging, and in many ways is reminiscent of *Six3-Cre;Lhx1*$^{lox/lox}$ SCN phenotypes (Roozendaal et al., 1987; Kawakami et al., 1997; Nakamura et al., 2011; Farajnia et al., 2012; Bedont et al, 2014; Bonaconsa et al., 2014). If the factors distinguishing consolidators from non-consolidators in our LPS paradigm could be worked out, temperature entrainment by moderate fever may present a potential tool for helping to reconsolidate rhythms in the elderly. Given a growing body of literature suggesting that circadian and sleep disruption presage a host of neurodegenerative and other ills as age advances in humans (Harper et al, 2004; Morton et al, 2005; Tranah et al, 2011), such an approach presents a potential low-cost intervention for managing the health of the graying population of the developed world.

We also used our mice as a tool for interrogating the neuropeptide dynamics of the SCN, utilizing cannulation studies. Induction of arrhythmicity in *Six3-Cre;Lhx1*$^{lox/lox}$ mice given i.c.v. Grp (Figure 3.6 B) suggests that whether a given neuropeptide promotes synchronization or desynchronization is not an intrinsic property of the molecule and its receptors alone. Instead, the effects of a given neuropeptide on synchrony also seem to depend on interpretation by the broader SCN neuropeptide network. It is known that large doses of Vip can transiently disrupt rhythms in normal mice, both in slice culture and in vivo, but that even very high doses of Grp fail to mimic this effect (An et al., 2013), and it has long been known that normal mice merely phase shift in response to exogenous Grp (Piggins et al., 1995). Based on the literature, one would expect excess Grp to help consolidate activity in Lhx1-deficient mice, as it does in slice cultures of *Vip*$^{-/-}$ SCN (Brown et al., 2005 and Maywood et al., 2011). Instead, quite the opposite occurs, suggesting that another signaling molecule(s) present in the *Vip*$^{-/-}$ SCN underpins Grp's synchrony-promoting activity.

Similarly, after i.c.v. Prok2 injection in *Six3-Cre;Lhx1*$^{lox/lox}$ mice, dramatic changes in not just phase-shift magnitude, as might be predicted when the SCN oscillator is damped (Vitaterna et al., 2006), but also period length (Figures 3.6 C–E) were surprising. This neuropeptide has no effect on phase or period in wild-type animals (Cheng et al., 2002), which we reproduce in our study. The dramatic differences in the effects of Prok2 infusion in wild-type and *Lhx1*-deficient mice indicate a previously unappreciated Lhx1-dependent role for the SCN in buffering changes in phase and period induced by infusion of SCN-derived output neuropeptides. This provides insight into a central problem faced by the SCN: how to prevent changes in the central oscillator

induced by both its own activity and afferent inputs from other brain regions, some of which use the same neurotransmitters, including Prok2 (Cheng et al., 2006 and Krout et al., 2002).

We propose that period buffering is at least partially mediated by the core neuropeptides Vip and Grp. Their mRNA expression negatively correlated with the magnitude of both phase and period changes after i.c.v. Prok2 infusion (data not shown), consistent with extending the peptides' well-documented ability to increase central oscillator robustness and thus control of circadian phase (Kuhlman et al., 2003, McArthur et al., 2000 and Piggins et al., 1995) to stabilization of circadian period in the face of perturbation by SCN output molecules. Meanwhile, expression of Avp positively correlated with both phase-shift magnitude and change in period length (data not shown), consistent with its role in relaying circadian clock signals to the SCN core (Leak and Moore, 2001 and Schwartz et al., 2010). To what extent the in vivo circadian system is susceptible to Prok2 infusion when only core neuropeptides are lost, as in the *Vip*$^{-/-}$ mouse, presents an interesting question for future study.

3.5 Contributions

Baseline Per2Luc studies were performed by Emily Slat. Clock gene ISH time-course was performed by Joseph Bedont. Baseline wheel running experiments were performed by Tara LeGates, as were pupil and optomotor studies, as well as EEG implantations and recordings for sleep studies. Preliminary analysis of EEG data was done by Tara LeGates; final analysis of EEG data was conducted by Dr. Valerie Mongrain. The X-gal study was done by Joseph Bedont. The choleratoxin study was done by Tara LeGates. Telemetry and wheel running temperature entrainment studies were conducted by Joseph

Bedont with assistance from Abhijith Bathini. The Per2Luc temperature resetting experiment was conducted by Dr. Ethan Buhr. Neuropeptide cannulation studies were performed by Dr. Mardi Byerly, with assistance from Tara LeGates and Joseph Bedont.

Chapter 4: General Summary and Conclusions

Large parts of this chapter are direct excerpts and/or paraphrased passages from Bedont et al, 2014 and Bedont and Blackshaw, 2015.

4.1 Findings of This Dissertation

Prior to our work of the last several years, cell-autonomous factors involved in the determination of SCN cell fate were essentially unknown. In the work described in Chapter 2, we identified Lhx1 as the first such factor necessary for the expression of a number of key neuropeptidergic fates by its cells, some of which seem to be controlled directly by Lhx1 (*Vip*, probably *Nms* and *Penk*), while others are controlled by Vip signaling (*Avp* and *Prok2*) or as-yet unidentified third parties (probably *Grp*) (Figures 2.2, 2.5, 4.1; Tables 2.1-2.2); Hatori et al, 2014. In comparison, expression of many genes induced earlier in development than these signals was intact, and though cell death occurs in the *Lhx1*-deficient SCN, this comes after the neuropeptide network is already

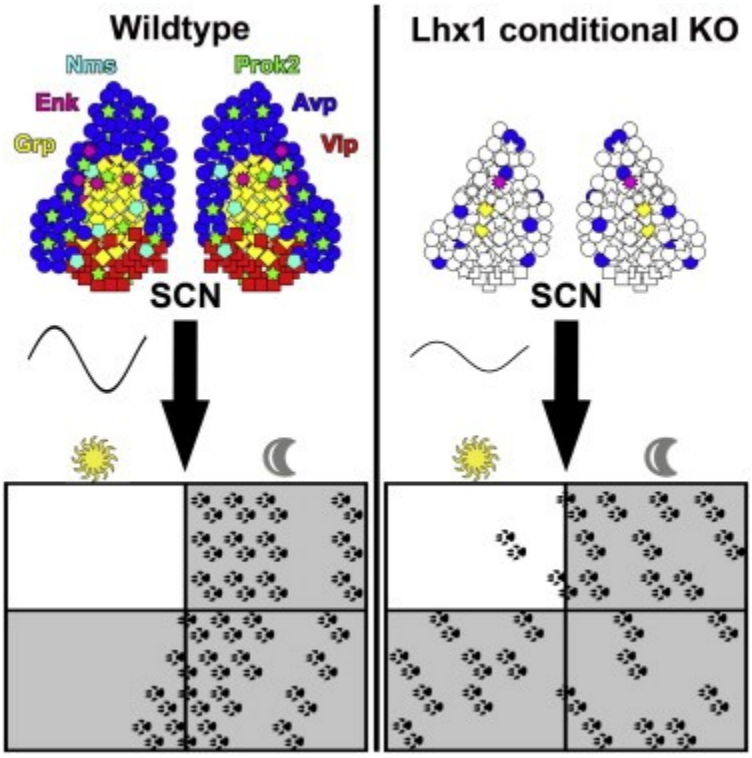

Figure 4.1: Graphical abstract of Bedont et al, 2014. This graphical abstract summarizes the main phenotypes of *Six3-Cre;Lhx1*$^{lox/lox}$ mice. **(1)** Loss of SCN neuropeptide expression. **(2)** Damping but not elimination of SCN cellular rhythms. **(3)** Modest LD but severe DD defects in circadian wheel-running behavior.

compromised (Figures 2.3, 2.4). Thus, Lhx1 appears to control terminal differentiation of the SCN. Considering the importance of many neuropeptides under its influence to the function of the adult SCN, this strongly implied that the developmental defects of *Six3-Cre;Lhx1*$^{lox/lox}$ mice would generate physiological phenotypes of general interest from a circadian perspective.

And indeed, as summed up in Chapter 3, this proved to be the case. Though our mutants showed SCN slice rhythms with surprisingly intact (albeit damped) amplitudes that appeared no more impaired than *Vip*$^{-/-}$ or *Vipr2*$^{-/-}$ mice (Figures 3.1, 4.1; Aton et al, 2005; Maywood et al, 2011), and wheel-running photoentrainment with a similarly modest set of defects (Figures 3.2, 4.1; Harmar et al, 2002; Colwell et al, 2003), their behavioral wheel-running rhythms in DD were markedly worse (Figures 3.2, 4.1; Harmar et al, 2002; Colwell et al, 2003). The photoentrainment and circadian distribution of vigilance states in our mutants was even more severe on a relative basis, appearing more similar to animals with complete SCN lesions than *Vip*$^{-/-}$ mice (Figure 3.3; Eastman et al, 1984; Hu et al, 2011). *Ankfn1*, lost in *Six3-Cre;Lhx1*$^{lox/lox}$ but not *Vip*$^{-/-}$ SCNs, is one promising candidate that may contribute to this difference, given the role of its Drosophila homolog in coupling the circadian clock to sleep (Figure 3.3 C; Liu et al, 2014).

Using these behaviors as a tool, we then used *Six3-Cre;Lhx1*$^{lox/lox}$ mice as a model for addressing unknown aspects of circadian function that are beyond the ability of single neuropeptide knockouts to interrogate. Our findings that *Six3-Cre;Lhx1*$^{lox/lox}$ but not *Vip*$^{-/-}$ mice selectively entrain to fever induced by LPS administration is the first major example, both showing the importance of the overall SCN neuropeptide network

dynamics for the resistance of SCN rhythms to temperature insults and providing the first direct *in vivo* evidence that this SCN resistance shown previously in culture is relevant on an organismal level (Figure 3.5; Buhr et al, 2010). Similarly, our cannulation studies with Grp and Prok2 were the first attempt at conducting these types of experiments in any genetic SCN neuropeptide-deficient model. Our findings suggest that the neuropeptide network is even more interdependent than previously appreciated, with the impact of a given cue highly dependent on the context of the network to have its usual circadian effects (Figure 3.6). Through these studies, we have gained novel insights into not just the development but also the physiology of the SCN, in areas that would have been difficult or impossible to explore employing more widely used single-neuropeptide knockout experiments.

4.2 Implications for SCN Development

Our work identified *Lhx1* as the first of what is no doubt many cell-autonomous regulators of SCN differentiation, given the region's highly heterogeneous patterns of gene expression. Leveraging this starting point, future investigations will be able to isolate both upstream regulators of *Lhx1* expression and downstream factors that further subdivide SCN neuropeptidergic populations. Combined with identification of factors involved in initial SCN specification, such as Six3, Six6, and Lhx2 (Clark et al., 2013, Roy et al., 2013 and VanDunk et al., 2011), this line of study could eventually allow stem cell lineages to be differentiated into specific SCN cell types.

This has great potential clinical relevance in the long term. iPSC-derived SCN transplants … represent a potential future cure for explicit disorders of the core circadian clock, as such transplants impart their period to the host's circadian behavior in animal

studies (Ralph et al., 1990). One such condition is familial advanced sleep phase disorder, a genetic ailment in which clock gene mutations disrupt the patient's internal period (reviewed in Nesbitt and Dijk, 2014). Such an intervention would free these patients from the constant need to rigidly structure their lives, in an effort to shoehorn their misaligned rhythms into following the solar cycle.

More generally, circadian disruption over the course of development in humans is very common. For instance, during adolescence the prevalence of formal delayed sleep phase disorder (DSPD) is estimated at ~7–16% (reviewed in Bartlett et al., 2013), and many teenagers that do not meet this formal diagnosis nonetheless tend toward a “night owl” chronotype. Coupled with social expectations out of phase with biological reality, this circadian change likely contributes to the incidence of psychiatric illness in adolescents, as DSPD and sometimes even the night owl chronotype alone have been linked to depression, obsessive-compulsive disorder, and other mental ailments (Lewy, 2009; Reid et al., 2012; Schubert and Coles, 2013). Early attempts at interventions in a military basic training environment have suggested that simply adapting adolescents' schedules to compensate for their altered chronotype improves sleep quality and learning, while ameliorating mood disturbance (Miller et al., 2012). A better understanding of SCN development may give insight into new approaches and tools for manipulating the circadian system for psychiatric effect during adolescence and at various other developmental stages.

Later in life, low amplitude and late phase of sleep/wake rhythms are predictive of problems such as dementia (Tranah et al., 2011) and progressive degradation of sleep/wake rhythms is apparent in both Alzheimer's and Huntington's disease (Harper et

al., 2004; Morton et al., 2005). Age-related circadian dysfunction likely stems at least partially from disruptions in SCN clock output; while core clock gene rhythms remain robust in the SCN throughout the lifespan in rodent models, output-related clock gene expression, electrical activity, and neuropeptide rhythms all decline with age (Roozendaal et al., 1987; Kawakami et al., 1997; Nakamura et al., 2011; Farajnia et al., 2012; Bonaconsa et al., 2014). Similar deficiencies have been noted in the aged human SCN, and many of these deficits are exacerbated in dementia patients, supporting the view that organic decline of the SCN contributes to the late-life sleep/wake fragmentation linked to neurodegeneration (reviewed in Hofman and Swaab, 2006). Understanding how various aspects of SCN output come online during development may give insight into how to restore them later in life, to combat this decline.

Finally, aside from neurodegenerative and psychiatric disease, circadian dysfunction is implicated in a host of metabolic and cardiovascular disorders in humans, as well as cancer and obesity (reviewed in Campos Costa et al., 2013; Froy, 2013; Videnovic et al., 2014; Virag and Lust, 2014; Masri et al., 2015). The ability to differentiate a human SCN from iPSCs will allow the modeling of such patients' central clock in culture, aiding in the identification of abnormalities in SCN function that may contribute to their pathology.

4.3 Implications for SCN Physiology

The insights into adult SCN physiology discovered using our developmental model as a tool also have potentially far-reaching implications for the circadian field. Our extension of the model of separable clock- and light-dependent pathways in the SCN from regulation of peripheral rhythms to also include regulation of vigilance state may

lead to a better understanding of how light directly influences sleep/wake cycles in humans. For a phenomenon so fundamental to our daily experience, this level of sleep regulation is shockingly poorly understood, and better comprehension of it may illuminate new strategies for exogenously manipulating our sleep cycles. One especially promising target, given our speculation on the mechanisms underlying *Six3-Cre;Lhx1*$^{lox/lox}$ sleep defects, is modulation of GABAergic signaling via Ankfn1 (Liu et al, 2014).

Given the age-related fragmentation of sleep rhythms and its relationship with neurodegenerative and other ills we have discussed previously, tools for restoring light regulation of sleep may offer a strategy for helping to maintain the health of our society's growing pool of elderly. Alternatively, if the consolidation of rhythms we sometimes see in our LPS experiments could be rendered more consistent with further study, periodic manipulations of core body temperature may offer another path derived from our work to reach the same goal of rhythm consolidation in the old. Many of the deficiencies we previously referenced in the aging SCN, such as loss of rhythms in output-related clock gene expression and neuropeptides, are reminiscent of *Six3-Cre;Lhx1*$^{lox/lox}$ mice, suggesting that such a strategy might well prove efficacious.

Finally, the complex interactions among neuropeptides revealed by our cannulation studies have intriguing potential uses for modulating the circadian system. For instance, it has previously been shown that a large dose of Vip but not Grp is able to accelerate re-entrainment of circadian rhythms after jetlag, despite the functional similarities of these signals in preserving synchrony and phase shifting intact rhythms in the circadian system (Piggins et al, 1995; Brown et al, 2005; Maywood et al, 2011; An et

al, 2013). However, our surprising finding of Grp-induced desynchrony in *Six3-Cre;Lhx1*$^{lox/lox}$ mice suggests that targeting multiple neuropeptidergic pathways may offer an additional route to accelerating circadian recovery from jetlag. In a similar vein, the period-lengthening effects of Prok2 in the presence of an otherwise inhibited SCN neuropeptide network may also offer an approach for pharmacologically treating familial advanced sleep phase disorder and other deficits of the circadian clock.

4.4 Future Directions and Final Reflection

Implicit in all of the potential uses of the developmental findings from our study is a pressing need for better understanding of the network as a whole. Our ongoing efforts to identify directly Lhx1-regulated and indirectly Vip-regulated genes in *Six3-Cre;Lhx1*$^{lox/lox}$ SCN is one step in this direction, but much more work remains to be done in elucidating the transcriptional network regulating SCN cell fate. The developmental roles of some factors recently implicated in regulating SCN-enriched gene expression, such as Creb3l1 and Zfhx3, have not yet been closely studied, but may represent additional factors influencing terminal differentiation of the SCN (Greenwood et al, 2014; Hatori et al, 2014; Parsons et al, 2015). A number of other transcription factors have spatiotemporal expression profiles that suggest roles in SCN development (Allen Brain Atlas; Shimogori et al, 2010; VanDunk et al, 2011). Myself and other members of the Blackshaw lab are currently studying some of these factors, and more will surely be investigated by others in coming years.

The precise basis of the insights into SCN physiology from our studies, such as which Lhx1-regulated genes control light regulation of sleep and resistance to temperature entrainment, represent another promising area for future studies. In order to

realize their clinical potential, a better understanding of the targets to pursue will first be necessary.

More generally, we also hope that the approach we have taken in my thesis will validate and encourage others to attack the adult physiology of the SCN from a developmental perspective. Though the targeting of single neuropeptides that the circadian field has largely pursued up to this point has and will continue to yield enormous contributions to our understanding of SCN network dynamics, we firmly believe that the combinatorial depletion of SCN signaling through developmental mutants like *Six3-Cre;Lhx1*$^{lox/lox}$ mice offer an invaluable complementary toolkit and perspective with great potential to help carry the field forward.

Chapter 5: References

1) Allen Brain Atlas (http://www.brain-map.org/).

2) Abe, M., Herzog, E.D., Yamazaki, S., Straume, M., Tei, H., Sakaki, Y., Menaker, M., and Block, G.D. (2002). Circadian rhythms in isolated brain regions. J. Neurosci. 22, 350-356.

3) Abizaid, A., Mezei, G., Sotonyi, P., and Horvath, T.L. (2004). Sex differences in adult suprachiasmatic nucleus neurons emerging late prenatally in rats. Eur. J. Neurosci. 19, 2488-2496.

4) Abrahamson, E.E., and Moore, R.Y. (2001). Suprachiasmatic nucleus in the mouse: retinal innervation, intrinsic organization and efferent projections. Brain Res. 916, 172-191.

5) Ahern, T.H., Krug, S., Carr, A.V., Murray, E.K., Fitzpatrick, E., Bengston, L., McCutcheon, J., De Vries, G.J., and Forger, N.G. (2013). Cell death atlas of the postnatal mouse ventral forebrain and hypothalamus: effects of age and sex. J. Comp. Neurol. 521, 2551-2569.

6) Albers, H.E., Liou, S.Y., Stopa, E.G., and Zoeller, R.T. (1991). Interaction of colocalized neuropeptides: functional significance in the circadian timing system. J. Neurosci. 11, 846-851.

7) Altman, J., and Bayer, S.A. (1978). Development of the diencephalon in the rat. I. Autoradiographic study of the time of origin and settling patterns of neurons of the hypothalamus. J. Comp. Neurol. 182, 945-971.

8) Alvarez-Bolado, G., Paul, F.A., and Blaess, S. (2012). Sonic hedgehog lineage in the mouse hypothalamus: from progenitor domains to hypothalamic regions. Neural Dev. 7, 4-8104-7-4.

9) An, S., Harang, R., Meeker, K., Granados-Fuentes, D., Tsai, C.A., Mazuski, C., Kim, J., Doyle, F.J.,3rd, Petzold, L.R., and Herzog, E.D. (2013). A neuropeptide speeds circadian entrainment by reducing intercellular synchrony. Proc. Natl. Acad. Sci. U. S. A. 110, E4355-61.

10) An, S., Irwin, R.P., Allen, C.N., Tsai, C., and Herzog, E.D. (2011). Vasoactive intestinal polypeptide requires parallel changes in adenylate cyclase and phospholipase C to entrain circadian rhythms to a predictable phase. J. Neurophysiol. 105, 2289-2296.

11) Antle, M.C., LeSauter, J., and Silver, R. (2005). Neurogenesis and ontogeny of specific cell phenotypes within the hamster suprachiasmatic nucleus. Brain Res. Dev. Brain Res. 157, 8-18.

12) Atkins, N.,Jr, Mitchell, J.W., Romanova, E.V., Morgan, D.J., Cominski, T.P., Ecker, J.L., Pintar, J.E., Sweedler, J.V., and Gillette, M.U. (2010). Circadian integration of glutamatergic signals by little SAAS in novel suprachiasmatic circuits. PLoS One 5, e12612.

13) Aton, S.J., Colwell, C.S., Harmar, A.J., Waschek, J., and Herzog, E.D. (2005). Vasoactive intestinal polypeptide mediates circadian rhythmicity and synchrony in mammalian clock neurons. Nat. Neurosci. 8, 476-483.

14) Bartlett, D.J., Biggs, S.N., and Armstrong, S.M. (2013). Circadian rhythm disorders among adolescents: assessment and treatment options. Med. J. Aust. 199, S16-20.

15) Bedont, J.L., and Blackshaw, S. (2015). Constructing the suprachiasmatic nucleus: a watchmaker's perspective on the central clockworks. Front. Syst. Neurosci. 9, 74.

16) Bedont, J.L., LeGates, T.A., Slat, E.A., Byerly, M.S., Wang, H., Hu, J., Rupp, A.C., Qian, J., Wong, G.W., Herzog, E.D., Hattar, S., and Blackshaw, S. (2014). Lhx1 controls terminal differentiation and circadian function of the suprachiasmatic nucleus. Cell. Rep. 7, 609-622.

17) Bedont, J.L., Newman, E.A., and Blackshaw, S. (2015). Patterning, specification, and differentiation in the developing hypothalamus. Wiley Interdiscip. Rev. Dev. Biol.

18) Bonaconsa, M., Malpeli, G., Montaruli, A., Carandente, F., Grassi-Zucconi, G., and Bentivoglio, M. (2014). Differential modulation of clock gene expression in the suprachiasmatic nucleus, liver and heart of aged mice. Exp. Gerontol. 55, 70-79.

19) Botchkina, G.I., and Morin, L.P. (1995). Ontogeny of radial glia, astrocytes and vasoactive intestinal peptide immunoreactive neurons in hamster suprachiasmatic nucleus. Brain Res. Dev. Brain Res. 86, 48-56.

20) Brohl, D., Strehle, M., Wende, H., Hori, K., Bormuth, I., Nave, K.A., Muller, T., and Birchmeier, C. (2008). A transcriptional network coordinately determines transmitter and peptidergic fate in the dorsal spinal cord. Dev. Biol. 322, 381-393.

21) Brooks, L.R., Chung, W.C., and Tsai, P.S. (2010). Abnormal hypothalamic oxytocin system in fibroblast growth factor 8-deficient mice. Endocrine 38, 174-180.

22) Brown, T.M., Colwell, C.S., Waschek, J.A., and Piggins, H.D. (2007). Disrupted neuronal activity rhythms in the suprachiasmatic nuclei of vasoactive intestinal polypeptide-deficient mice. J. Neurophysiol. 97, 2553-2558.

23) Brown, T.M., Hughes, A.T., and Piggins, H.D. (2005). Gastrin-releasing peptide promotes suprachiasmatic nuclei cellular rhythmicity in the absence of vasoactive intestinal polypeptide-VPAC2 receptor signaling. J. Neurosci. 25, 11155-11164.

24) Buhr, E.D., and Takahashi, J.S. (2013). Molecular components of the Mammalian circadian clock. Handb. Exp. Pharmacol. (217):3-27. doi, 3-27.

25) Buhr, E.D., Yoo, S.H., and Takahashi, J.S. (2010). Temperature as a universal resetting cue for mammalian circadian oscillators. Science 330, 379-385.

26) Campos Costa, I., Nogueira Carvalho, H., and Fernandes, L. (2013). Aging, circadian rhythms and depressive disorders: a review. Am. J. Neurodegener Dis. 2, 228-246.

27) Cepeda-Nieto, A.C., Pfaff, S.L., and Varela-Echavarria, A. (2005). Homeodomain transcription factors in the development of subsets of hindbrain reticulospinal neurons. Mol. Cell. Neurosci. 28, 30-41.

28) Chen, S.K., Badea, T.C., and Hattar, S. (2011). Photoentrainment and pupillary light reflex are mediated by distinct populations of ipRGCs. Nature 476, 92-95.

29) Cheng, M.Y., Bullock, C.M., Li, C., Lee, A.G., Bermak, J.C., Belluzzi, J., Weaver, D.R., Leslie, F.M., and Zhou, Q.Y. (2002). Prokineticin 2 transmits the behavioural circadian rhythm of the suprachiasmatic nucleus. Nature 417, 405-410.

30) Clark, D.D., Gorman, M.R., Hatori, M., Meadows, J.D., Panda, S., and Mellon, P.L. (2013). Aberrant development of the suprachiasmatic nucleus and circadian rhythms in mice lacking the homeodomain protein Six6. J. Biol. Rhythms 28, 15-25.

31) Colwell, C.S., Michel, S., Itri, J., Rodriguez, W., Tam, J., Lelievre, V., Hu, Z., Liu, X., and Waschek, J.A. (2003). Disrupted circadian rhythms in VIP- and PHI-deficient mice. Am. J. Physiol. Regul. Integr. Comp. Physiol. 285, R939-49.

32) Crossland, W.J., and Uchwat, C.J. (1982). Neurogenesis in the central visual pathways of the golden hamster. Brain Res. 281, 99-103.

33) Davis, F.C., Boada, R., and LeDeaux, J. (1990). Neurogenesis of the hamster suprachiasmatic nucleus. Brain Res. 519, 192-199.

34) Delville, Y., Mansour, K.M., Quan, E.W., Yules, B.M., and Ferris, C.F. (1994). Postnatal development of the vasopressinergic system in golden hamsters. Brain Res. Dev. Brain Res. 81, 230-239.

35) Eastman, C.I., Mistlberger, R.E., and Rechtschaffen, A. (1984). Suprachiasmatic nuclei lesions eliminate circadian temperature and sleep rhythms in the rat. Physiol. Behav. 32, 357-368.

36) El Helou, J., Belanger-Nelson, E., Freyburger, M., Dorsaz, S., Curie, T., La Spada, F., Gaudreault, P.O., Beaumont, E., Pouliot, P., Lesage, F.*, et al.* (2013). Neuroligin-1 links neuronal activity to sleep-wake regulation. Proc. Natl. Acad. Sci. U. S. A. 110, 9974-9979.

37) Farajnia, S., Michel, S., Deboer, T., vanderLeest, H.T., Houben, T., Rohling, J.H., Ramkisoensing, A., Yasenkov, R., and Meijer, J.H. (2012). Evidence for neuronal desynchrony in the aged suprachiasmatic nucleus clock. J. Neurosci. 32, 5891-5899.

38) Froy, O. (2013). Circadian aspects of energy metabolism and aging. Ageing Res. Rev. 12, 931-940.

39) Furuta, Y., Lagutin, O., Hogan, B.L., and Oliver, G.C. (2000). Retina- and ventral forebrain-specific Cre recombinase activity in transgenic mice. Genesis 26, 130-132.

40) Gamble, K.L., Allen, G.C., Zhou, T., and McMahon, D.G. (2007). Gastrin-releasing peptide mediates light-like resetting of the suprachiasmatic nucleus circadian pacemaker through cAMP response element-binding protein and Per1 activation. J. Neurosci. 27, 12078-12087.

41) Geusz, M.E., Fletcher, C., Block, G.D., Straume, M., Copeland, N.G., Jenkins, N.A., Kay, S.A., and Day, R.N. (1997). Long-term monitoring of circadian rhythms in c-fos gene expression from suprachiasmatic nucleus cultures. Curr. Biol. 7, 758-766.

42) Goecks, J., Nekrutenko, A., Taylor, J., and Galaxy Team. (2010). Galaxy: a comprehensive approach for supporting accessible, reproducible, and transparent computational research in the life sciences. Genome Biol. 11, R86-2010-11-8-r86. Epub 2010 Aug 25.

43) Greenwood, M., Bordieri, L., Greenwood, M.P., Rosso Melo, M., Colombari, D.S., Colombari, E., Paton, J.F., and Murphy, D. (2014). Transcription factor CREB3L1 regulates vasopressin gene expression in the rat hypothalamus. J. Neurosci. 34, 3810-3820.

44) Guler, A.D., Ecker, J.L., Lall, G.S., Haq, S., Altimus, C.M., Liao, H.W., Barnard, A.R., Cahill, H., Badea, T.C., Zhao, H.*, et al.* (2008). Melanopsin cells are the principal conduits for rod-cone input to non-image-forming vision. Nature 453, 102-105.

45) Harmar, A.J., Marston, H.M., Shen, S., Spratt, C., West, K.M., Sheward, W.J., Morrison, C.F., Dorin, J.R., Piggins, H.D., Reubi, J.C.*, et al.* (2002). The VPAC(2)

receptor is essential for circadian function in the mouse suprachiasmatic nuclei. Cell 109, 497-508.

46) Harper, D.G., Stopa, E.G., McKee, A.C., Satlin, A., Fish, D., and Volicer, L. (2004). Dementia severity and Lewy bodies affect circadian rhythms in Alzheimer disease. Neurobiol. Aging 25, 771-781.

47) Hatori, M., Gill, S., Mure, L.S., Goulding, M., O'Leary, D.D., and Panda, S. (2014). Lhx1 maintains synchrony among circadian oscillator neurons of the SCN. Elife (Cambridge) e03357.

48) Hattar, S., Liao, H.W., Takao, M., Berson, D.M., and Yau, K.W. (2002). Melanopsin-containing retinal ganglion cells: architecture, projections, and intrinsic photosensitivity. Science 295, 1065-1070.

49) Herzog, E.D., Aton, S.J., Numano, R., Sakaki, Y., and Tei, H. (2004). Temporal precision in the mammalian circadian system: a reliable clock from less reliable neurons. J. Biol. Rhythms 19, 35-46.

50) Herzog, E.D., Grace, M.S., Harrer, C., Williamson, J., Shinohara, K., and Block, G.D. (2000). The role of Clock in the developmental expression of neuropeptides in the suprachiasmatic nucleus. J. Comp. Neurol. 424, 86-98.

51) Hofman, M.A., and Swaab, D.F. (2006). Living by the clock: the circadian pacemaker in older people. Ageing Res. Rev. 5, 33-51.

52) Hu, J., Hu, H., and Li, X. (2008). MOPAT: a graph-based method to predict recurrent cis-regulatory modules from known motifs. Nucleic Acids Res. 36, 4488-4497.

53) Husse, J., Leliavski, A., Tsang, A.H., Oster, H., and Eichele, G. (2014). The light-dark cycle controls peripheral rhythmicity in mice with a genetically ablated suprachiasmatic nucleus clock. FASEB J. 28, 4950-4960.

54) Kabrita, C.S., and Davis, F.C. (2008). Development of the mouse suprachiasmatic nucleus: determination of time of cell origin and spatial arrangements within the nucleus. Brain Res. 1195, 20-27.

55) Kawakami, F., Okamura, H., Tamada, Y., Maebayashi, Y., Fukui, K., and Ibata, Y. (1997). Loss of day-night differences in VIP mRNA levels in the suprachiasmatic nucleus of aged rats. Neurosci. Lett. 222, 99-102.

56) Kawamoto, K., Nagano, M., Kanda, F., Chihara, K., Shigeyoshi, Y., and Okamura, H. (2003). Two types of VIP neuronal components in rat suprachiasmatic nucleus. J. Neurosci. Res. 74, 852-857.

57) Krout, K.E., Kawano, J., Mettenleiter, T.C., and Loewy, A.D. (2002). CNS inputs to the suprachiasmatic nucleus of the rat. Neuroscience 110, 73-92.

58) Kuhlman, S.J., Silver, R., Le Sauter, J., Bult-Ito, A., and McMahon, D.G. (2003). Phase resetting light pulses induce Per1 and persistent spike activity in a subpopulation of biological clock neurons. J. Neurosci. 23, 1441-1450.

59) Kwan, K.M., and Behringer, R.R. (2002). Conditional inactivation of Lim1 function. Genesis 32, 118-120.

60) Leak, R.K., and Moore, R.Y. (2001). Topographic organization of suprachiasmatic nucleus projection neurons. J. Comp. Neurol. 433, 312-334.

61) Lee, I.T., Chang, A.S., Manandhar, M., Shan, Y., Fan, J., Izumo, M., Ikeda, Y., Motoike, T., Dixon, S., Seinfeld, J.E., Takahashi, J.S., and Yanagisawa, M. (2015).

Neuromedin s-producing neurons act as essential pacemakers in the suprachiasmatic nucleus to couple clock neurons and dictate circadian rhythms. Neuron 85, 1086-1102.

62) Lewy, A.J. (2009). Circadian misalignment in mood disturbances. Curr. Psychiatry Rep. 11, 459-465.

63) Li, J.D., Burton, K.J., Zhang, C., Hu, S.B., and Zhou, Q.Y. (2009). Vasopressin receptor V1a regulates circadian rhythms of locomotor activity and expression of clock-controlled genes in the suprachiasmatic nuclei. Am. J. Physiol. Regul. Integr. Comp. Physiol. 296, R824-30.

64) Li, J.D., Hu, W.P., Boehmer, L., Cheng, M.Y., Lee, A.G., Jilek, A., Siegel, J.M., and Zhou, Q.Y. (2006). Attenuated circadian rhythms in mice lacking the prokineticin 2 gene. J. Neurosci. 26, 11615-11623.

65) Liu, S., Lamaze, A., Liu, Q., Tabuchi, M., Yang, Y., Fowler, M., Bharadwaj, R., Zhang, J., Bedont, J., Blackshaw, S.*, et al.* (2014). WIDE AWAKE mediates the circadian timing of sleep onset. Neuron 82, 151-166.

66) Masri, S., Kinouchi, K., and Sassone-Corsi, P. (2015). Circadian clocks, epigenetics, and cancer. Curr. Opin. Oncol. 27, 50-56.

67) Massart, R., Freyburger, M., Suderman, M., Paquet, J., El Helou, J., Belanger-Nelson, E., Rachalski, A., Koumar, O.C., Carrier, J., Szyf, M., and Mongrain, V. (2014). The genome-wide landscape of DNA methylation and hydroxymethylation in response to sleep deprivation impacts on synaptic plasticity genes. Transl. Psychiatry. 4, e347.

68) Maywood, E.S., Chesham, J.E., O'Brien, J.A., and Hastings, M.H. (2011). A diversity of paracrine signals sustains molecular circadian cycling in suprachiasmatic nucleus circuits. Proc. Natl. Acad. Sci. U. S. A. 108, 14306-14311.

69) McArthur, A.J., Coogan, A.N., Ajpru, S., Sugden, D., Biello, S.M., and Piggins, H.D. (2000). Gastrin-releasing peptide phase-shifts suprachiasmatic nuclei neuronal rhythms in vitro. J. Neurosci. 20, 5496-5502.

70) Miller, N.L., Tvaryanas, A.P., and Shattuck, L.G. (2012). Accommodating adolescent sleep-wake patterns: the effects of shifting the timing of sleep on training effectiveness. Sleep 35, 1123-1136.

71) Mirochnik, V., Bosler, O., Tillet, Y., Calas, A., and Ugrumov, M. (2005). Long-lasting effects of serotonin deficiency on differentiating peptidergic neurons in the rat suprachiasmatic nucleus. Int. J. Dev. Neurosci. 23, 85-91.

72) Moore, R.Y., and Bernstein, M.E. (1989). Synaptogenesis in the rat suprachiasmatic nucleus demonstrated by electron microscopy and synapsin I immunoreactivity. J. Neurosci. 9, 2151-2162.

73) Moore, R.Y., and Eichler, V.B. (1972). Loss of a circadian adrenal corticosterone rhythm following suprachiasmatic lesions in the rat. Brain Res. 42, 201-206.

74) Morin, L.P., Blanchard, J., and Moore, R.Y. (1992). Intergeniculate leaflet and suprachiasmatic nucleus organization and connections in the golden hamster. Vis. Neurosci. 8, 219-230.

75) Morton, A.J., Wood, N.I., Hastings, M.H., Hurelbrink, C., Barker, R.A., and Maywood, E.S. (2005). Disintegration of the sleep-wake cycle and circadian timing in Huntington's disease. J. Neurosci. 25, 157-163.

76) Muller, C., and Torrealba, F. (1998). Postnatal development of neuron number and connections in the suprachiasmatic nucleus of the hamster. Brain Res. Dev. Brain Res. 110, 203-213.

77) Munekawa, K., Tamada, Y., Iijima, N., Hayashi, S., Ishihara, A., Inoue, K., Tanaka, M., and Ibata, Y. (2000). Development of astroglial elements in the suprachiasmatic nucleus of the rat: with special reference to the involvement of the optic nerve. Exp. Neurol. 166, 44-51.

78) Nakamura, T.J., Nakamura, W., Yamazaki, S., Kudo, T., Cutler, T., Colwell, C.S., and Block, G.D. (2011). Age-related decline in circadian output. J. Neurosci. 31, 10201-10205.

79) Nesbitt, A.D., and Dijk, D.J. (2014). Out of synch with society: an update on delayed sleep phase disorder. Curr. Opin. Pulm. Med. 20, 581-587.

80) Okamura, H.S., Murakami, K., Uda, T., Sugano, Y., Takahashi, C., Yanaihara, N., and Ibata, Y. (1986). Coexistence of vasoactive intestinal peptide (VIP)-, peptide histidine isoleucine amide (PHI)-, and gastrin releasing peptide (GRP)-like immunoreactivity in neurons of the rat suprachiasmatic nucleus. Biomed. Res. 7, 295-299.

81) Parsons, M.J., Brancaccio, M., Sethi, S., Maywood, E.S., Satija, R., Edwards, J.K., Jagannath, A., Couch, Y., Finelli, M.J., Smyllie, N.J.*, et al.* (2015). The Regulatory Factor ZFHX3 Modifies Circadian Function in SCN via an AT Motif-Driven Axis. Cell 162, 607-621.

82) Piggins, H.D., Antle, M.C., and Rusak, B. (1995). Neuropeptides phase shift the mammalian circadian pacemaker. J. Neurosci. 15, 5612-5622.

83) Pillai, A., Mansouri, A., Behringer, R., Westphal, H., and Goulding, M. (2007). Lhx1 and Lhx5 maintain the inhibitory-neurotransmitter status of interneurons in the dorsal spinal cord. Development 134, 357-366.

84) Poche, R.A., Kwan, K.M., Raven, M.A., Furuta, Y., Reese, B.E., and Behringer, R.R. (2007). Lim1 is essential for the correct laminar positioning of retinal horizontal cells. J. Neurosci. 27, 14099-14107.

85) Prosser, H.M., Bradley, A., Chesham, J.E., Ebling, F.J., Hastings, M.H., and Maywood, E.S. (2007). Prokineticin receptor 2 (Prokr2) is essential for the regulation of circadian behavior by the suprachiasmatic nuclei. Proc. Natl. Acad. Sci. U. S. A. 104, 648-653.

86) Pulivarthy, S.R., Tanaka, N., Welsh, D.K., De Haro, L., Verma, I.M., and Panda, S. (2007). Reciprocity between phase shifts and amplitude changes in the mammalian circadian clock. Proc. Natl. Acad. Sci. U. S. A. 104, 20356-20361.

87) Ralph, M.R., Foster, R.G., Davis, F.C., and Menaker, M. (1990). Transplanted suprachiasmatic nucleus determines circadian period. Science 247, 975-978.

88) Redlin, U., and Mrosovsky, N. (1999). Masking by light in hamsters with SCN lesions. J. Comp. Physiol. A. 184, 439-448.

89) Reid, K.J., Jaksa, A.A., Eisengart, J.B., Baron, K.G., Lu, B., Kane, P., Kang, J., and Zee, P.C. (2012). Systematic evaluation of Axis-I DSM diagnoses in delayed sleep phase disorder and evening-type circadian preference. Sleep Med. 13, 1171-1177.

90) Romero, M.T., and Silver, R. (1990). Time course of peptidergic expression in fetal suprachiasmatic nucleus transplanted into adult hamster. Brain Res. Dev. Brain Res. 57, 1-6.

91) Roozendaal, B., van Gool, W.A., Swaab, D.F., Hoogendijk, J.E., and Mirmiran, M. (1987). Changes in vasopressin cells of the rat suprachiasmatic nucleus with aging. Brain Res. 409, 259-264.

92) Roy, A., de Melo, J., Chaturvedi, D., Thein, T., Cabrera-Socorro, A., Houart, C., Meyer, G., Blackshaw, S., and Tole, S. (2013). LHX2 is necessary for the maintenance of optic identity and for the progression of optic morphogenesis. J. Neurosci. 33, 6877-6884.

93) Schindelin, J., Arganda-Carreras, I., Frise, E., Kaynig, V., Longair, M., Pietzsch, T., Preibisch, S., Rueden, C., Saalfeld, S., Schmid, B.*, et al.* (2012). Fiji: an open-source platform for biological-image analysis. Nat. Methods 9, 676-682.

94) Schubert, J.R., and Coles, M.E. (2013). Obsessive-compulsive symptoms and characteristics in individuals with delayed sleep phase disorder. J. Nerv. Ment. Dis. 201, 877-884.

95) Schwartz, M.D., Congdon, S., and de la Iglesia, H.O. (2010). Phase misalignment between suprachiasmatic neuronal oscillators impairs photic behavioral phase shifts but not photic induction of gene expression. J. Neurosci. 30, 13150-13156.

96) Shawlot, W., and Behringer, R.R. (1995). Requirement for Lim1 in head-organizer function. Nature 374, 425-430.

97) Shen, H., Glass, J.D., Seki, T., and Watanabe, M. (1999). Ultrastructural analysis of polysialylated neural cell adhesion molecule in the suprachiasmatic nuclei of the adult mouse. Anat. Rec. 256, 448-457.

98) Shen, H., Watanabe, M., Tomasiewicz, H., Rutishauser, U., Magnuson, T., and Glass, J.D. (1997). Role of neural cell adhesion molecule and polysialic acid in mouse circadian clock function. J. Neurosci. 17, 5221-5229.

99) Shimogori, T., Lee, D.A., Miranda-Angulo, A., Yang, Y., Wang, H., Jiang, L., Yoshida, A.C., Kataoka, A., Mashiko, H., Avetisyan, M*., et al.* (2010). A genomic atlas of mouse hypothalamic development. Nat. Neurosci. 13, 767-775.

100) Silver, R., LeSauter, J., Tresco, P.A., and Lehman, M.N. (1996). A diffusible coupling signal from the transplanted suprachiasmatic nucleus controlling circadian locomotor rhythms. Nature 382, 810-813.

101) Slat, E., Freeman, G.M.,Jr, and Herzog, E.D. (2013). The clock in the brain: neurons, glia, and networks in daily rhythms. Handb. Exp. Pharmacol. (217):105-23. doi, 105-123.

102) Southey, B.R., Lee, J.E., Zamdborg, L., Atkins, N.,Jr, Mitchell, J.W., Li, M., Gillette, M.U., Kelleher, N.L., and Sweedler, J.V. (2014). Comparing label-free quantitative peptidomics approaches to characterize diurnal variation of peptides in the rat suprachiasmatic nucleus. Anal. Chem. 86, 443-452.

103) Speh, J.C., and Moore, R.Y. (1993). Retinohypothalamic tract development in the hamster and rat. Brain Res. Dev. Brain Res. 76, 171-181.

104) Stephan, F.K., and Zucker, I. (1972). Circadian rhythms in drinking behavior and locomotor activity of rats are eliminated by hypothalamic lesions. Proc. Natl. Acad. Sci. U. S. A. 69, 1583-1586.

105) Tranah, G.J., Blackwell, T., Stone, K.L., Ancoli-Israel, S., Paudel, M.L., Ensrud, K.E., Cauley, J.A., Redline, S., Hillier, T.A., Cummings, S.R., Yaffe, K., and SOF Research Group. (2011). Circadian activity rhythms and risk of incident dementia and mild cognitive impairment in older women. Ann. Neurol. 70, 722-732.

106) Trapnell, C., Hendrickson, D.G., Sauvageau, M., Goff, L., Rinn, J.L., and Pachter, L. (2013). Differential analysis of gene regulation at transcript resolution with RNA-seq. Nat. Biotechnol. 31, 46-53.

107) Tsai, P.S., Brooks, L.R., Rochester, J.R., Kavanaugh, S.I., and Chung, W.C. (2011). Fibroblast growth factor signaling in the developing neuroendocrine hypothalamus. Front. Neuroendocrinol. 32, 95-107.

108) Ugrumov, M.V., Trembleau, A., and Calas, A. (1994). Altered vasoactive intestinal polypeptide gene expression in the fetal rat suprachiasmatic nucleus following prenatal serotonin deficiency. Int. J. Dev. Neurosci. 12, 143-149.

109) Vacher, C.M., Fretier, P., Creminon, C., Seif, I., De Maeyer, E., Calas, A., and Hardin-Pouzet, H. (2003). Monoaminergic control of vasopressin and VIP expression in the mouse suprachiasmatic nucleus. J. Neurosci. Res. 71, 791-801.

110) VanDunk, C., Hunter, L.A., and Gray, P.A. (2011). Development, maturation, and necessity of transcription factors in the mouse suprachiasmatic nucleus. J. Neurosci. 31, 6457-6467.

111) Videnovic, A., Lazar, A.S., Barker, R.A., and Overeem, S. (2014). 'The clocks that time us'-circadian rhythms in neurodegenerative disorders. Nat. Rev. Neurol.

112) Virag, J.A., and Lust, R.M. (2014). Circadian influences on myocardial infarction. Front. Physiol. 5, 422.

113) Vitaterna, M.H., Ko, C.H., Chang, A.M., Buhr, E.D., Fruechte, E.M., Schook, A., Antoch, M.P., Turek, F.W., and Takahashi, J.S. (2006). The mouse Clock mutation reduces circadian pacemaker amplitude and enhances efficacy of resetting stimuli and phase-response curve amplitude. Proc. Natl. Acad. Sci. U. S. A. 103, 9327-9332.

114) Yamaguchi, Y., Suzuki, T., Mizoro, Y., Kori, H., Okada, K., Chen, Y., Fustin, J.M., Yamazaki, F., Mizuguchi, N., Zhang, J.*, et al.* (2013). Mice genetically deficient in vasopressin V1a and V1b receptors are resistant to jet lag. Science 342, 85-90.

115) Zhao, Y., Kwan, K.M., Mailloux, C.M., Lee, W.K., Grinberg, A., Wurst, W., Behringer, R.R., and Westphal, H. (2007). LIM-homeodomain proteins Lhx1 and Lhx5, and their cofactor Ldb1, control Purkinje cell differentiation in the developing cerebellum. Proc. Natl. Acad. Sci. U. S. A. 104, 13182-13186.

Chapter 6: Curriculum Vitae

6.1 Liberal Arts and Secondary Eduction

Johns Hopkins Medical Institute (Baltimore, MD)

PhD in Neuroscience, expected October 2015.

University of Rochester (Rochester, NY)

BS in Neuroscience and BA in Psychology with a Minor in Chemistry (May 2009).

6.2 Laboratory and Research Experience

Johns Hopkins Medical Institute (Baltimore, MD)

- Graduate Student in Prof. Seth Blackshaw's Lab (April 2010-present). Characterizing the gene expression and behavioral phenotype in the suprachiasmatic nucleus of targeted Lim homeodomain factor 1 knock-out mice. Also, leveraging this model to explore circadian physiology, and as a starting point to dissect the pathways guiding suprachiasmatic nucleus development.
- Rotation Student in Prof. Randy Reed's Lab (January 2010-March 2010). Using real-time PCR to examine transcriptional repression of mutant olfactory receptors in cellulo.
- Rotation Student in Prof. Michael Caterina's Lab (October 2009-December 2009). Attempting to design calcium and/or phosphoinositide imaging assays for high throughput characterization of TRPV1 pore expansion mutant in cellulo.
- Rotation Student in Prof. Nicholas Marsh-Armstrong's Lab (July 2009-September 2009). Utilizing a laser photocoagulation mouse model of glaucoma and in situ hybridization to investigate the role of gamma-synuclein in the disease.

Strong Memorial Hospital (Rochester, NY)

■ Research Assistant in Prof. Julie Fudge's Lab (September 2008-May 2009). Using immunocytochemistry and Neurolucida analysis of tract tracing to study NE receptor distribution on extended amygdala projections to substantia nigra. Studies designed to assess how this innervation might affect the dopamine system.

■ Research Assistant in Prof. Robert Freeman's Lab (September 2007-May 2008). Permanently transfected fusion proteins into eukaryotic cell lines and created plasmids encoding novel fusion proteins. Studies designed to produce an assay for EGLN activity.

■ Technical Assistant in Prof. Benjamin Segal's Lab (September 2006-May 2007). Genotyped and managed rodent colony and sterilized instruments.

New York University Center for Neural Science (New York City, NY)

■ Summer Undergraduate Researcher in Prof. Joseph LeDoux's Lab (June 2008-August 2008). Analyzed serial electron micrographs of lateral amygdalas taken from rats exposed to different fear learning paradigms. Study designed to evaluate changes in spine apparatuses and other organelles in dendrites in response to fear learning.

University of Pittsburgh Center for Neuroscience (Pittsburgh, PA)

■ Summer Undergraduate Researcher in Prof. Gonzalo Torres's Lab (June 2007-August 2007). Used Western blotting, PCR, and uptake assays to examine effects of dopamine transporter (DAT) polymorphisms in peripheral lymphocytes, with the goal of finding a peripheral marker predictive of schizophrenia. A side project looked for a D3 receptor / DAT protein-protein interaction.

6.3 Research Publications

■ Bedont JL, LeGates TA, Buhr E, Bathini A, Ling J, Wong P, Van Gelder R, Hattar S, Mongrain V, and Blackshaw S. "Vip-independent effects of Lhx1 in the suprachiasmatic nucleus." (in preparation)

■ Bedont JL & Blackshaw S. "Constructing the suprachiasmatic nucleus: a watchmaker's perspective on the central clockworks." (2015). Frontiers in Systems Neuroscience 9:74.

■ Bedont JL, Newman E, & Blackshaw S. "Development of the hypothalamus: from patterning to differentiation." (2015). Wiley Interdisciplinary Reviews 4(5): 445-68.

■ Salvatierra J, Lee DA, Zibetti C, Duran M, Yoo S, Newman EA, Wang H, Bedont JL, de Melo J, Miranda-Angulo A, Aja S, Garcia S, Garcia-Verdugo JM, & Blackshaw S. "The LIM homeodomain factor Lhx2 is required for hypothalamic tanycyte specification and differentiation." (2014). Journal of Neuroscience 34(50): 16809-20.

■ Bedont JL, Legates TA, Slat EA, Byerly MS, Wang H, Hu J, Rupp AC, Qian J, Wong GW, Herzog ED, Hattar S, & Blackshaw S. "Lhx1 controls terminal differentiation and circadian function of the suprachiasmatic nucleus." (2014). Cell Reports 7(3): 609-22.

■ Liu S, Lamaze A, Liu Q, Tabuchi M, Yang Y, Fowler M, Bharadwaj R, Zhang J, Bedont J, Blackshaw S, Lloyd TE, Montell C, Sehgal A, Koh K, & Wu MN. "WIDE AWAKE mediates the circadian timing of sleep onset." (2014). Neuron 82(1): 151-66.

■ Lee DA, Bedont JL, Pak T, Wang H, Song J, Miranda-Angulo A, Takiar V, Charubhumi V, Balordi F, Takebayashi H, Aja S, Ford E, Fishell G, & Blackshaw S.. "Tanycytes of the hypothalamic median eminence form a diet-responsive neurogenic niche." (2012.) Nature Neuroscience 15(5): 700-2.

■ Nguyen J, Soto I, Keun-Young K, Bushong E, Oglesby E, Valiente-Soriano F, Yang Z, Davis C, Bedont J, Son J, Wei J, Buchman V, Zack D, Vidal-Sanz M, Ellisman M, Marsh-Armstrong N. "Myelination transition zone astrocytes internalize axonal evulsions and increase reactivity in response to glaucoma synucleinopathy." (2011). PNAS 108: 1176-81, 2011.

■ Ostroff L, Cain C, Bedont J, Monfils M, & LeDoux J. "Fear and safety learning differentially affect synapse size and dendritic translation in the lateral amygdala." (2010). PNAS 107(20): 9418-23.

6.4 Research Presentations

- "Vip-Independent Effects of the Lhx1-Controlled Transcriptional Network in the Suprachiasmatic Nucleus." Bedont J, LeGates T, Buhr E, Slat E, Bathini A, Herzog E, Van Gelder R, Hattar S, Mongrain V, & Blackshaw S. Janelia Research Conference: Hypothalamic Circuits for Control of Survival Behaviors, September 2015 [Poster Presentation].
- "Vip-Independent Effects of the Lhx1-Controlled Transcriptional Network in the Suprachiasmatic Nucleus." Bedont J, LeGates T, Buhr E, Slat E, Bathini A, Herzog E, Van Gelder R, Hattar S, Mongrain V, & Blackshaw S. Gordon Chronobiology Research Conference and Seminar, June 2015 [Poster Presentations].
- "Developmental defects in the Lhx1-deficient SCN give insight into circadian physiology." Bedont J, LeGates T, Slat E, Byerly M, Wang H, Wong W, Herzog E, Hattar S, & Blackshaw S. Society for Neuroscience Conference, November 2014 [Nanosymposium Talk].
- "Lhx1: from studies of SCN differentiation to insights into SCN physiology." Bedont J, LeGates T, Slat E, Byerly M, Wang H, Wong W, Herzog E, Hattar S, & Blackshaw S. Society for Research in Biological Rhythms Research Conference, June 2014 [Symposium Talk].
- "Lhx1 is required for differentiation and function of the mouse suprachiasmatic nucleus." Bedont J, LeGates T, Slat E, Byerly M, Wang H, Hu J, Qiang J, Wong W Herzog E, Hattar S, & Blackshaw S. Society for Neuroscience Conference, November 2013 [Nanosymposium Talk].

■ “Lhx1 is required for differentiation and function of the mouse suprachiasmatic nucleus.” Bedont J, LeGates T, Slat E, Wang H, Hu J, Qiang J, Herzog E, Hattar S, & Blackshaw S. Gordon Neural Development Research Conference, August 2012 [Poster Presentation].

■ “Lhx1 is required for differentiation and function of the mouse suprachiasmatic nucleus.” Bedont J, LeGates T, Slat E, Wang H, Hu J, Qiang J, Herzog E, Hattar S, & Blackshaw S. Society for Research in Biological Rhythms Research Conference, June 2012 [Symposium Talk].

■ “Lhx1 is required for differentiation and function of the mouse suprachiasmatic nucleus.” Bedont J, LeGates T, Wang H, Hattar S, & Blackshaw S. Gordon Chronobiology Research Conference, June 2011 [Poster Presentation].

6.5 Fellowships and Awards

- JHMI Graduate Student Association Travel Award (2015)
- Alicia Showalter Reynolds Young Investigator Award (2015)
- Society for Research in Biological Rhythms Research Excellence Award (2014)
- First Prize at the Annual Johns Hopkins Neuroscience Department Retreat Poster Session (2013)
- Society for Neuroscience Graduate Student Travel Award (2013)
- National Science Foundation Innovation in Graduate Education Challenge Semifinalist (2013)
- Society for Research in Biological Rhythms Research Merit Award (2012)
- National Science Foundation Graduate Research Fellowship (2011)
- Wilmer Eye Institute Visual Neuroscience Training Program Fellowship (2010)
- National Science Foundation Graduate Research Fellowship Honorable Mention (2010)
- Kort Fellowship (2009)

6.6 Teaching Experience

■ Head of the Project Bridge Pedagogy Committee (Fall 2013-Spring 2015). As head of this committee, I guided the selection of facilitators and preparation for four interactive workshops aimed at helping scientists better engage the public about their science.

■ NSF RISE Experimental Design and Statistics Workshop (Summer 2010-Summer 2014). With the assistance of Drs. Christine Hohmann and Michael Koban, I designed from scratch and facilitated an interactive weeklong workshop geared at helping prepare undergraduates from Morgan State Univeristy (an HBCU in the Baltimore area) to better engage intellectually in research experiences they were paired with through the NSF RISE program. The workshop was continually improved in accordance with the prior year's experience during each of the five years I ran it. I also trained a younger graduate student in the pedagogy necessary to carry on the workshop and provided progressive scaffolding to prepare her for taking over the workshop beginning two years before my departure.

■ Co-Teaching "Emerging Strategies in Innate Behaviors" with Drs. Seth Blackshaw and Samer Hattar (Spring 2013). I directly taught four interactive lecture / paper discussions in this upper level elective course, and assisted as desired in all other lecture / discussions. I also wrote all exams and carried out most evaluation for papers and exams for the course.

■ TA for Cell Physiology Workshops for First-Year Medical Students (Fall 2012-2013). I assisted two different professors in running interactive workshop sessions for first-year medical students after their lectures each day for an ~2 week long period in the fall.

■ Workshop Leader for Organic Chemistry Workshops (Fall 2007-Spring 2009). I ran an interactive weekly workshop for 8-10 University of Rochester undergraduates each semester. This was paired with a weekly pedagogy course and personalized feedback to improve our performance as facilitators for our workshops. As a "Super Leader" my senior year, I also helped to run these pedagogy training sessions.